University of Dundee

Discovery of soticlestat, a potent and selective inhibitor for cholesterol 24-hydroxylase (CH24H)

Koike, Tatsuki; Yoshikawa, Masato; Ando, Haruhi Kamisaki; Farnaby, William; Nishi, Toshiya; Watanabe, Etsurou

Article

Discovery of Soticlestat, a Potent and Selective Inhibitor for Cholesterol 24-Hydroxylase (CH24H)

Tatsuki Koike,* Masato Yoshikawa, Haruhi Kamisaki Ando, William Farnaby, Toshiya Nishi, Etsurou Watanabe, Jason Yano, Maki Miyamoto, Shigeru Kondo, Tsuyoshi Ishii, and Takanobu Kuroita

ACCESS | 📊 Metrics & More | 📰 Article Recommendations | 🅢ℹ️ Supporting Information

ABSTRACT: Cholesterol 24-hydroxylase (CH24H, CYP46A1), a brain-specific cytochrome P450 (CYP) family enzyme, plays a role in the homeostasis of brain cholesterol by converting cholesterol to 24S-hydroxycholesterol (24HC). Despite a wide range of potential of CH24H as a drug target, no potent and selective inhibitors have been identified. Here, we report on the structure-based drug design (SBDD) of novel 4-arylpyridine derivatives based on the X-ray co-crystal structure of hit derivative **1b**. Optimization of 4-arylpyridine derivatives led us to identify **3v** ((4-benzyl-4-hydroxypiperidin-1-yl)(2,4′-bipyridin-3-yl)methanone, IC_{50} = 7.4 nM) as a highly potent, selective, and brain-penetrant CH24H inhibitor. Following oral administration to mice, **3v** resulted in a dose-dependent reduction of 24HC levels in the brain (1, 3, and 10 mg/kg). Compound **3v** (soticlestat, also known as TAK-935) is currently under clinical investigation for the treatment of Dravet syndrome and Lennox-Gastaut syndrome as a novel drug class for epilepsies.
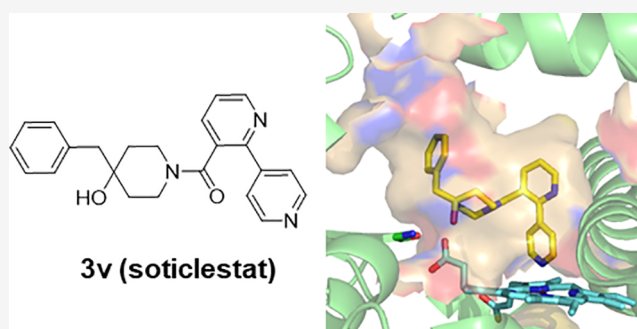
INTRODUCTION

CYP46A1, also known as cholesterol 24-hydroxylase (CH24H), is a brain-specific cytochrome P450 (CYP) family enzyme that converts cholesterol to 24S-hydroxycholesterol (24HC) and plays a role in the homeostasis of brain cholesterol.[1] It has been reported that polymorphism in the CH24H gene is associated with the risk of Alzheimer's disease (AD).[2,3] In AD patients, 24HC levels in cerebrospinal fluid (CSF) are elevated compared with healthy control,[4−6] and the expression of CH24H is reported to be increased in the reactive astrocyte and results in disruption of the glial glutamate transporter EAAT2 association with lipid rafts.[7] The potential role of CH24H in glutamate regulation was also supported in our previous study.[8] It is also suggested that 24HC is involved in the regulation of various receptors such as the liver X receptors,[9] estrogen receptors,[10] retinoid orphan receptors,[11] and N-methyl-D-aspartate (NMDA) receptors.[12] This mounting evidence links CH24H with various neurological diseases[2−6,8,13] such as AD and epilepsy.

The therapeutic potential of CH24H activation has been extensively investigated;[14−19] however, inhibitors of the CH24H enzyme have not been fully studied as a central nervous system (CNS) drug target. Recently, we reported that soticlestat (also known as TAK-935, Figure 1), developed as a potent and selective inhibitor for CH24H, shows therapeutic potential for diseases associated with neural hyperexcitation in mice.[8] Soticlestat is currently being investigated as a drug for treatment of Dravet syndrome (DS) and Lennox-Gastaut

syndrome (LGS) with a novel mechanism of action.[20−22] In this paper, we report the design, synthesis, and discovery of soticlestat starting from a high-throughput screening (HTS) campaign, followed by further optimization utilizing structure-based drug design (SBDD).

To design and develop therapeutic CH24H inhibitor, not only the potent CH24H inhibitory activity but also the selectivity over off-target CYPs is essential because CYP family enzymes are broadly responsible for drug metabolism as well as hormone synthesis.[23] In recent years, crystal structures have been reported for substrate-bound and substrate-free CH24H,[24] and for the CH24H complex with some marketed drugs such as the antifungal agent voriconazole.[25,26] Although voriconazole is reported to reduce brain 24HC,[27−29] the pharmacological effects are also attributable to other mechanisms in the mevalonate pathway, given the voriconazole activity of CYP51 inhibition. Therefore, it was important to identify a potent, highly selective and brain-penetrant CH24H inhibitor that merits clinical and preclinical investigation into the therapeutic potential of the central CH24H inhibition. Since no potent and selective CH24H inhibitors have been
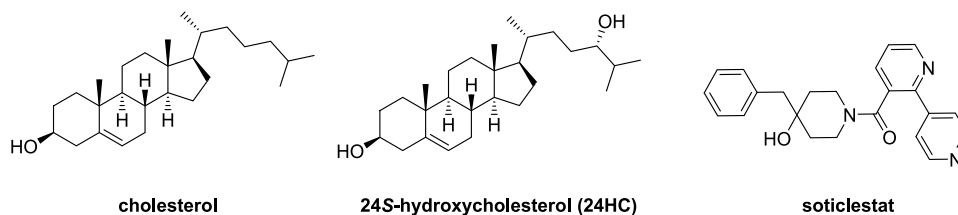
Figure 1. Chemical structures of cholesterol, 24S-hydroxycholesterol (24HC), and soticlestat.
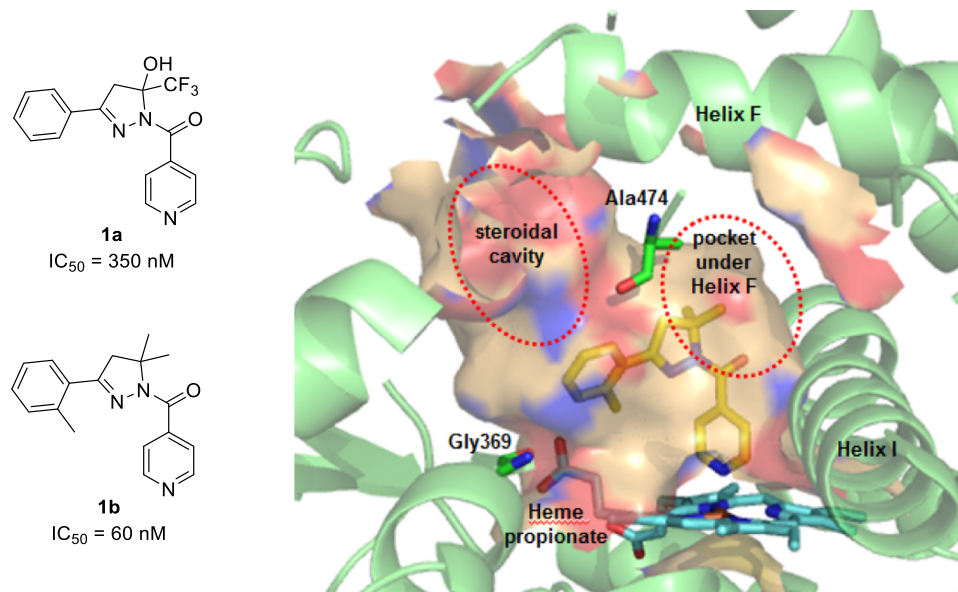
Figure 2. Chemical structure of hit compound **1a** and X-ray co-crystal structure of CH24H with hit derivative **1b** (PDB ID 7LS4).
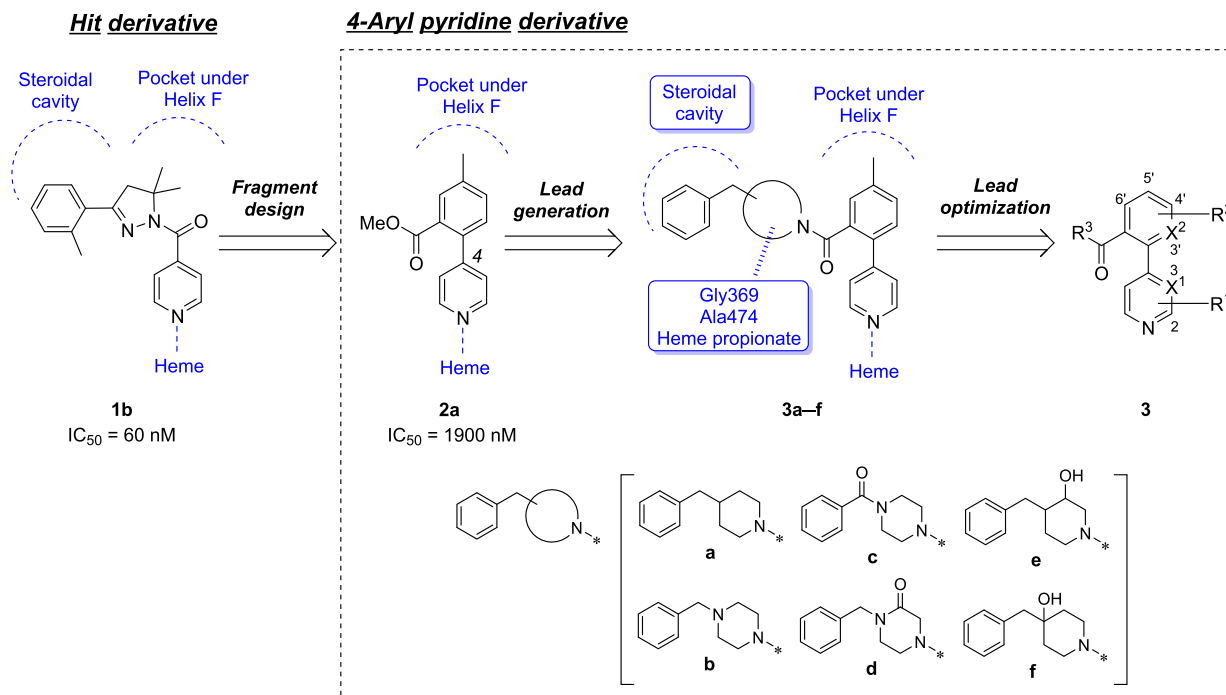
Figure 3. Scaffold hopping to find potent and selective CH24H inhibitors.

described in publication so far, we performed HTS campaign, where human CH24H inhibitory activities were evaluated by measuring the amount of $[^{14}C]$ 24HC produced from $[^{14}C]$ cholesterol in the CH24H-expressed cell lysate. As a result, compound **1a** was identified with moderate CH24H inhibitory activity (IC$_{50}$ = 350 nM, Figure 2), whereas voriconazole did not show an activity potent enough for determination of IC$_{50}$ (>10 000 nM). Subsequent structure−activity relationship

Scheme 1

4a: R^2=5'-Me, R^4=Me
4b: R^2=5'-Cl, R^4=Me
4c: R^2=5'-MeO, R^4=Me
4d: R^2=5'-F, R^4=Me
4e: R^2=H, R^4=Et

2a: R^2=5'-Me, R^4=Me
2b: R^2=5'-Cl, R^4=Me
2c: R^2=5'-MeO, R^4=Me
2d: R^2=5'-F, R^4=Me
2e: R^2=H, R^4=Et

2f: R^2=5'-Me
2g: R^2=5'-Cl
2h: R^2=5'-MeO
2i: R^2=5'-F
2j: R^2=H

4f   **6**   **7**   **2k**

4g   **8**   **2l**
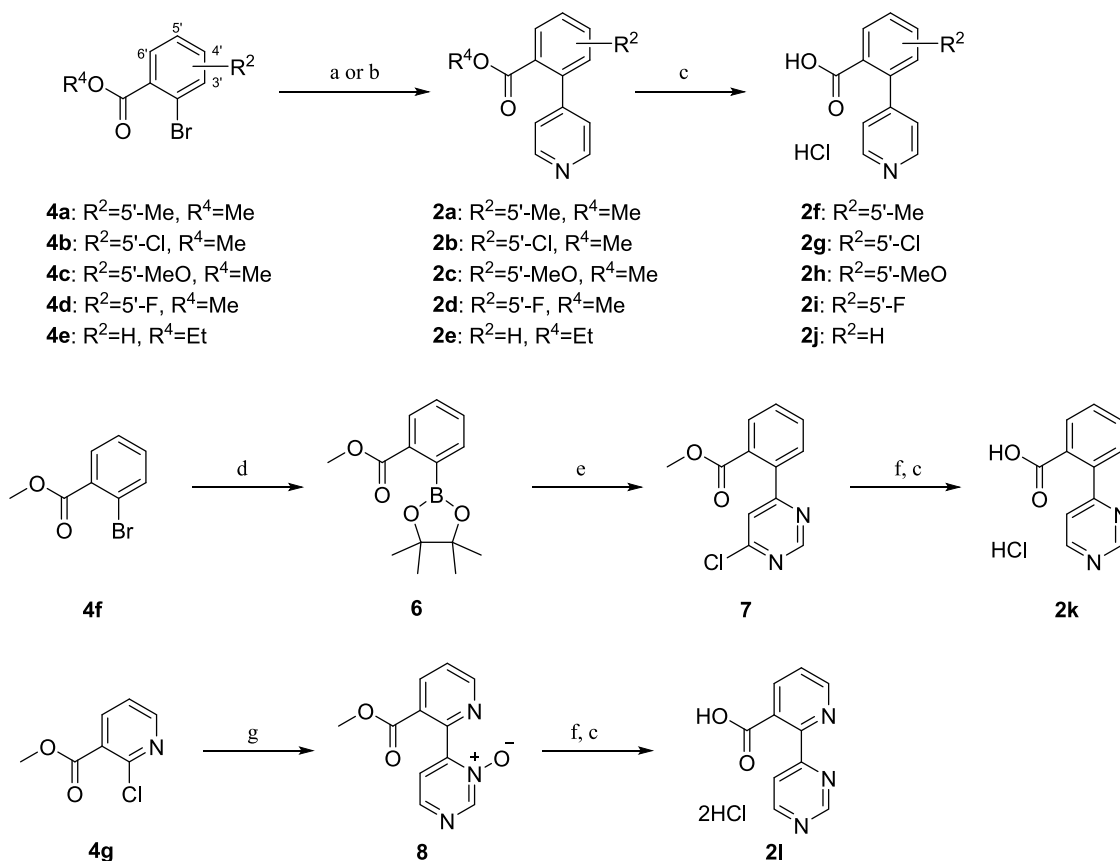
[a]Reagents and conditions: (a) Pd(PPh$_3$)$_4$, Na$_2$CO$_3$, 4-pyridineboronic acid **5a**, DME/water, reflux, overnight; (b) Pd(PPh$_3$)$_4$, Na$_2$CO$_3$, **5a**, DME/water, MW 140 °C, 1 h; (c) 6 M HCl aq. AcOH, reflux, 5 h–overnight; (d) Pd(dppf)Cl$_2$/CH$_2$Cl$_2$, KOAc, bis(pinacolato)diboron, THF/DMSO (20:1), 80 °C, 5 h; (e) Pd(PPh$_3$)$_4$, Na$_2$CO$_3$, 4,6-dichloropyrimidine, DME/water, MW 150 °C, 1 h; (f) 10% Pd-C, Et$_3$N, MeOH, H$_2$, rt, 1 h; (g) Pd(OAc)$_2$, t-Bu$_3$P/HBF$_4$, CuCN, K$_2$CO$_3$, pyrimidine N-oxide, 1,4-dioxane, MW 150 °C, 2 h.

(SAR) studies identified compound **1b** with improved CH24H inhibitory activity (IC$_{50}$ = 60 nM), and the co-crystal structure of compound **1b** with CH24H was obtained (Figure 2). Compound **1b** is shown to bind in the active site of CH24H with direct ligation to the heme iron by its pyridine nitrogen at a distance of 2.0 Å. In addition to ligation to heme, hydrophobic interactions such as an interaction with a pocket under Helix F by the dimethyl moiety of compound **1b** was revealed to be important.

This co-crystal structure of compound **1b** with CH24H inspired us to design 4-arylpyridine derivatives as novel CH24H inhibitors (Figure 3). 4-Arylpyridine was designed as a rigid and effective fragment that makes two important interactions: one is the direct ligation to the heme iron by its pyridine nitrogen and the other is the hydrophobic interaction with the pocket under Helix F by its aryl moiety. To validate this hypothesis, methyl 5-methyl-2-(pyridine-4-yl) benzoate **2a** was designed and synthesized. Compound **2a** showed CH24H inhibitory activity (IC$_{50}$ = 1900 nM), suggesting that the 4-arylpyridine could be a novel fragment for further CH24H inhibitor design.

Introduction of a substituent on the ester moiety of compound **2a** was designed to improve CH24H inhibitory activity. Co-crystal structure of compound **1b** with CH24H indicates that CH24H has several residues around the active site such as Gly369, Ala474, and heme propionate, which can make further hydrogen bonds with the ligand. In addition to

these hydrogen-bonding interactions, we also focused on a hydrophobic interaction with a large hydrophobic cavity, in which the steroidal scaffold of cholesterol is placed when acting as a substrate (steroidal cavity). To obtain these additional interactions, we designed compounds **3a** and **3b** which have 4-benzylpiperidine amide or 4-benzylpiperazine amide as a substituent (Figure 3). A benzyl group on the 4-position of piperidine or piperazine can access the steroidal cavity as a hydrophobic substituent. In addition to this hydrophobic interaction, introduction of a carbonyl group (**3c**, **3d**) as a hydrogen bond acceptor (HBA) or a hydroxyl group (**3e**, **3f**) as a hydrogen bond donor (HBD) on the piperidine or piperazine ring was designed to form additional interaction with Gly369, Ala474, or heme propionate.

■ RESULTS AND DISCUSSION

Chemistry. The syntheses of the biarylcarboxylic acids **2f–l** are illustrated in Scheme 1. Compounds **2a–e** were obtained by Suzuki coupling reaction of commercially available 2-bromobenzoates **4a–e** with 4-pyridineboronic acid **5a**. Hydrolysis of **2a–e** in the presence of hydrochloric acid afforded acids **2f–j** as HCl salts. Compound **2k** was obtained starting from commercially available 2-bromomethylbenzoate **4f**. Compound **4f** was converted to boronic ester **6** by the borylation reaction using bis(pinacolato)diboron and Pd-(dppf)Cl$_2$. Suzuki coupling reaction of compound **6** with 4,6-dichloropyrimidine, followed by hydrogenation and

Scheme 2

3a: X^1=CH, X^2=CH, R^2=5'-Me, R^3=**9a**
3d: X^1=CH, X^2=CH, R^2=5'-Me, R^3=**9d**
3e: X^1=CH, X^2=CH, R^2=5'-Me, R^3=**9e**
3f: X^1=CH, X^2=CH, R^2=5'-Me, R^3=**9f**
3h: X^1=CH, X^2=CH, R^2=5'-Me, R^3=**9h**
3i: X^1=CH, X^2=CH, R^2=5'-Me, R^3=**9i**
3q: X^1=CH, X^2=CH, R^2=5'-Cl, R^3=**9f**
3r: X^1=CH, X^2=CH, R^2=5'-OMe, R^3=**9f**
3s: X^1=CH, X^2=CH, R^2=5'-F, R^3=**9f**
3u: X^1=N, X^2=CH, R^2=H, R^3=**9f**
3w: X^1=CH, X^2=CH, R^2=H, R^3=**9k**
3x: X^1=N, X^2=N, R^2=H, R^3=**9f**
3z: X^1=N, X^2=CH, R^2=H, R^3=**9k**
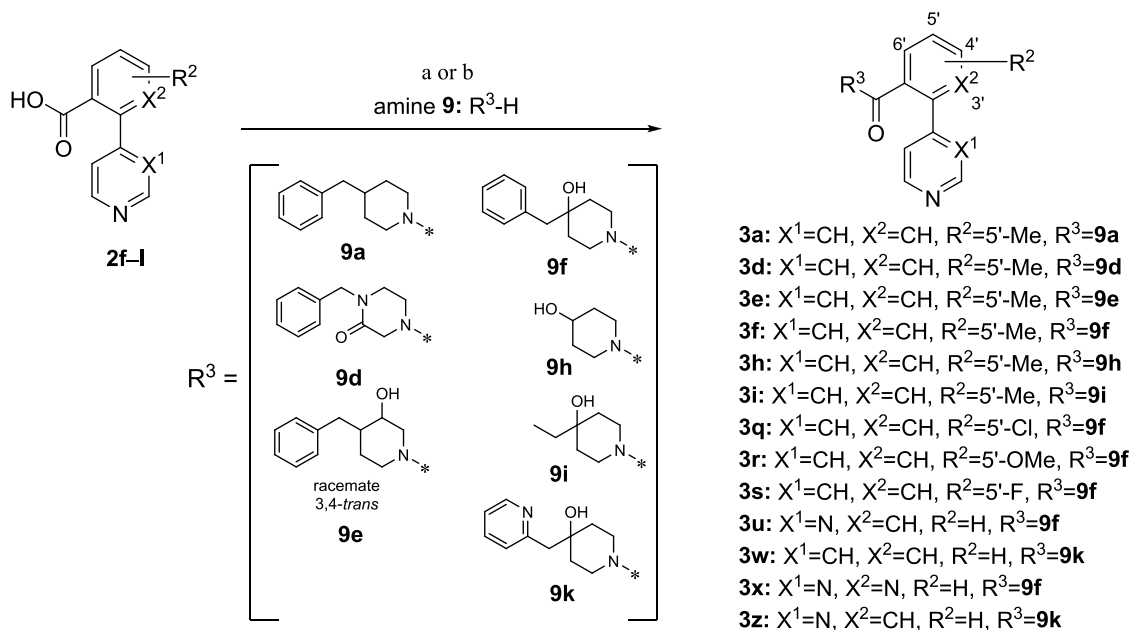
[a]Reagents and conditions: (a) DMT-MM, amine **9**, DMF, rt, 3 h−overnight; (b) HATU, Et₃N, **9**, DMF, rt, overnight.

Scheme 3

10a: X^2=CH, R^2=5'-Me, Hal=Br, R^3=**9f**
10b: X^2=CH, R^2=5'-Me, Hal=Br, R^3=**9g**
10c: X^2=CH, R^2=5'-Me, Hal=Br, R^3=**9j**
10d: X^2=CH, R^2=3'-Me, Hal=Br, R^3=**9f**
10e: X^2=CH, R^2=4'-Me, Hal=Br, R^3=**9f**
10f: X^2=CH, R^2=6'-Me, Hal=Br, R^3=**9f**
10g: X^2=CH, R^2=H, Hal=Br, R^3=**9f**
10h: X^2=N, R^2=H, Hal=Cl, R^3=**9f**
10i: X^2=N, R^2=H, Hal=Cl, R^3=**9k**

3g: X^2=CH, R^1=H, R^2=5'-Me, R^3=**9g**
3j: X^2=CH, R^1=H, R^2=5'-Me, R^3=**9j**
3k: X^2=CH, R^1=2-Me, R^2=5'-Me, R^3=**9f**
3l: X^2=CH, R^1=3-F, R^2=5'-Me, R^3=**9f**
3m: X^2=CH, R^1=3-Me, R^2=5'-Me, R^3=**9f**
3n: X^2=CH, R^1=H, R^2=3'-Me, R^3=**9f**
3o: X^2=CH, R^1=H, R^2=4'-Me, R^3=**9f**
3p: X^2=CH, R^1=H, R^2=6'-Me, R^3=**9f**
3t: X^2=CH, R^1=H, R^2=H, R^3=**9f**
3v: X^2=N, R^1=H, R^2=H, R^3=**9f**
3y: X^2=N, R^1=H, R^2=H, R^3=**9k**

[a]Reagents and conditions: (a) DMT-MM, amine **9**, DMF, rt, 2 days; (b) HATU, Et₃N, **9**, DMF, rt, overnight; (c) oxalyl chloride, DMF (cat.), toluene, rt; Et₃N, **9**, THF, rt, overnight; (d) Thionyl chloride, DMF, DME, 90 °C; Et₃N, **9**, THF, rt, overnight; (e) NaH, MeI, DMF, 0 °C to rt; (f) Pd(PPh₃)₄, Na₂CO₃, pyridineboronic acids **5**, DME/water, MW 120 or 140 °C, 1 h; (g) Pd(PPh₃)₄, Na₂CO₃, **5**, DMF/water, 100 °C, overnight; (h) Pd(dppf)₂Cl₂·CH₂Cl₂, 2 M Na₂CO₃, **5**, diglyme, 120 °C, overnight.

hydrolysis, afforded compound **2k** as the HCl salt. Compound **2l** was obtained as the di-HCl salt by the coupling reaction of commercially available methyl 2-chloropyridine-3-carboxylate **4g** and pyrimidine *N*-oxide,[30] followed by hydrogenation and hydrolysis.

Compounds **3a**, **3d−f**, **3h**, **3i**, **3q−s**, **3u**, **3w**, **3x**, and **3z** were obtained by the amide coupling reaction of acids **2f−l** with commercially available amines **9** using 4-(4,6-dimethoxy-1,3,5-triazin-2-yl)-4-methylmorpholinium chloride (DMT-MM) or (dimethylamino)-*N*,*N*-dimethyl(3*H*-[1,2,3]triazolo[4,5-*b*]-

Scheme 4

[a]Reagents and conditions: (a) HATU, Et$_3$N, t-butylpiperadine-1-carboxylate, DMF, rt, overnight; (b) Pd(PPh$_3$)$_4$, Na$_2$CO$_3$, 4-pyridineboronic acids **5a**, DME/water, MW 150 °C, 1 h; (c) HCl, EtOAc, rt, overnight; (d) NaBH(OAc)$_3$, benzaldehyde, EtOAc, rt, overnight; (e) HATU, DIPEA, benzoic acid, DMF, rt, overnight.

pyridine-3-yloxy)-methaniminium hexafluorophosphate (HATU) as condensation agents (Scheme 2).

Compounds **3g**, **3j−p**, **3t**, **3v**, and **3y** were obtained by the amide coupling reaction of commercially available acids **4h−m** with amines **9** using DMT-MM or HATU as condensation agents followed by Suzuki coupling reaction with 4-pyridineboronic acid **5a−d** (Scheme 3).

Compounds **3b** and **3c** were obtained starting from 2-bromo-5-methylbenzoic acid **4h**. Compound **4h** was coupled with t-butylpiperazine-1-carboxylate using HATU to generate compound **11**, followed by Suzuki coupling reaction with 4-pyridineboronic acid **5a** and deprotection with hydrochloric acid to afford compound **12** (Scheme 4). Compound **3b** was obtained by the reductive amination of compound **12** with benzaldehyde. Compound **3c** was obtained by the amide coupling of compound **12** with benzoic acid.

Lead Generation by Exploration of Heterocyclic Amide. The results for the human CH24H inhibitory activities of 5-methyl-2-(pyridine-4-yl)benzamide derivatives **3a−j** are shown in Table 1.

4-Benzylpiperidine derivative **3a** (IC$_{50}$ = 110 nM) and 4-benzylpiperazine derivative **3b** (IC$_{50}$ = 93 nM) showed improved CH24H inhibitory activities compared with that of the lead fragment **2a** (IC$_{50}$ = 1900 nM). These results suggested that the benzyl group on the 4-position of piperidine or piperazine ring could access the steroidal cavity to make a hydrophobic interaction in addition to the heme coordination and hydrophobic interaction by the biaryl scaffold. We then explored an additional interaction with the enzyme by adding an HBA or HBD on the piperidine or piperazine ring. Piperazine amide derivative **3c** (IC$_{50}$ > 10 000 nM) and piperazinone derivative **3d** (IC$_{50}$ = 89 nM), in which the carbonyl group was added as an HBA, did not show increased activities compared with that of the nonsubstituted compound **3b** (IC$_{50}$ = 93 nM). On the other hand, introduction of a hydroxyl group on the 3-position (**3e**, IC$_{50}$ = 16 nM) and the 4-position (**3f**, IC$_{50}$ = 2.7 nM) of the piperidine ring resulted in a significant increase of the CH24H inhibitory activities compared with that of the nonsubstituted compound **3a** (IC$_{50}$ = 110 nM). These results suggested that a new hydrogen bonding with Gly369, Ala474, or heme propionate could be obtained by adding a hydroxyl group as an HBD in the ligand.

In fact, methylation of the hydroxyl group on compound **3f** gives about 30 times decrease in activity (**3g**, IC$_{50}$ = 74 nM).

Next, the effect of the benzyl group on CH24H inhibition was investigated by changing the 4-benzyl group on the piperidine ring while keeping the 4-hydroxyl group on the piperidine. Removal of the benzyl group (**3h**, IC$_{50}$ = 7700 nM) and the replacement of the benzyl group with ethyl (**3i**, IC$_{50}$ = 540 nM) or phenyl (**3j**, IC$_{50}$ = 1200 nM) groups resulted in a decrease in CH24H inhibitory activity. These results suggested that the 4-benzyl group on the piperidine ring could access the steroidal cavity to form hydrophobic interactions with appropriate distance from the active site. As a result, we could identify 4-hydroxyl-4-benzylpiperidine as a promising substituent to form additional interactions with CH24H from a 4-arylpyridine scaffold.

Compound **3f** was selected as the lead compound for further optimization, and its co-crystal structure with CH24H was obtained (Figure 4). Our design concept has been validated by confirming the four key interactions of compound **3f** with CH24H; that is, direct ligation to the heme iron by pyridine nitrogen, hydrophobic interaction with the pocket under Helix F by a tolyl moiety, hydrophobic interaction with the steroidal cavity by a benzyl group, and a hydrogen bond between Gly369 and the hydroxyl group. With these features, compound **3f** demonstrated in vitro nanomolar CH24H inhibitory activity for the human CH24H enzyme.

Lead Optimization of the Biaryl Scaffold. Having identified 4-hydroxyl-4-benzylpiperidine as a promising substituent on the 4-arylpyridine scaffold, we then looked to optimize the 4-arylpyridine moiety starting from lead compound **3f**. CH24H inhibitory activities as well as the calculated lipophilicity ($c \log P$) and CYP3A4 inhibitory activities (% inhibition at 10 μM) for each compound are shown in Table 2.

Introduction of a methyl group on the 2-position of the pyridine ring resulted in a pronounced decrease in the CH24H inhibitory activity (**3k**, IC$_{50}$ > 10 000 nM), suggesting that the methyl group next to the pyridine nitrogen prevented formation of a ligand to the heme iron. Introduction of a fluoro group on the 3-position of the pyridine ring slightly diminished the CH24H inhibitory activity (**3l**, IC$_{50}$ = 17 nM), while a methyl group maintained the activity (**3m**, IC$_{50}$ = 4.9 nM). These results indicate that the electron-withdrawing

Table 1. Inhibitory Activities of 3a–j for Human CH24H Enzyme[a,b]

Cpd	R^3	CH24H[a] IC$_{50}$ (nM)[b]
3a		110 (71 – 180)
3b		93 (41 – 210)
3c		>10000
3d		89 (17 – 460)
3e	3,4-*trance*, racemate	16 (9.4 – 26)
3f		2.7 (1.8 – 4.2)
3g		74 (44 – 120)
3h		7700 (3600 – 16000)
3i		540 (330 – 880)
3j		1200 (850 – 1700)

[a]Human enzyme. [b]IC$_{50}$ values and 95% confidence intervals (given in parentheses) were calculated from duplicate measurements by a four-parameter logistic curve using XLfit software (IDBS, London, UK).

fluoride lowers the heme ligation ability of the pyridine nitrogen.

We then obtained SAR on the benzene ring of the biaryl scaffold. Introduction of a methyl group on the 3′-position of the benzene ring resulted in a decrease in the CH24H inhibitory activity (3n, IC$_{50}$ = 130 nM), suggesting that the methyl group on the 3′-position is not tolerated because of the steric conflict with Helix I of CH24H (Figure 4). On the other hand, introduction of a methyl group on the 4′-position (3o, IC$_{50}$ = 4.4 nM) and 6′-position (3p, IC$_{50}$ = 7.8 nM) of the
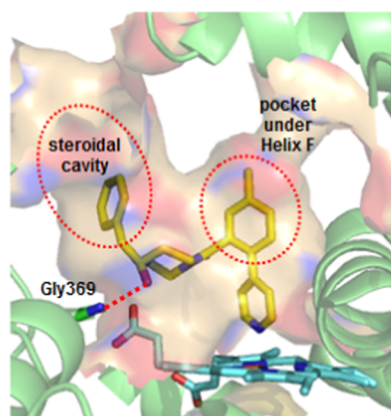
Figure 4. X-ray co-crystal structure of CH24H with **3f** (PDB ID 7LS3).

Table 2. CH24H Inhibitory Activities, Calculated Lipophilicity ($c \log P$), and CYP3A4 Inhibitory Activities of Compounds 3f and 3k−t

Cpd	R^1	R^2	$c \log P^c$	CH24H[a] IC_{50} (nM)[b]	CYP3A4 % (10 μM)
3f	H	5'-Me	2.8	2.7 (1.8−4.2)	67
3k	2-Me	5'-Me	3.3	>10 000	60
3l	3-F	5'-Me	3.0	17 (13−21)	77
3m	3-Me	5'-Me	3.0	4.9 (2.6−9.2)	91
3n	H	3'-Me	2.5	130 (65−260)	77
3o	H	4'-Me	2.8	4.4 (2.5−7.5)	65
3p	H	6'-Me	2.8	7.8 (5.4−11)	71
3q	H	5'-Cl	3.0	2.4 (1.7−3.5)	75
3r	H	5'-OMe	2.5	4.7 (2.2−10)	67
3s	H	5'-F	2.5	6.1 (4.0−9.2)	55
3t	H	H	2.3	7.9 (2.6−24)	45

[a]Human enzyme. [b]IC_{50} values and 95% confidence intervals (given in parentheses) were calculated from duplicate measurements using a four-parameter logistic curve using XLfit software (IDBS, London, UK). [c]Calculated $\log P$ values were obtained using Daylight.[31]

benzene ring maintained CH24H inhibitory activity. SAR of the 5'-position of the benzene ring was also obtained. Replacement of the methyl group of compound **3f** (IC_{50} = 2.7 nM) with chloro (**3q**, IC_{50} = 2.4 nM), methoxy (**3r**, IC_{50} = 4.7 nM), and fluoro (**3s**, IC_{50} = 6.1 nM) groups maintained the CH24H inhibitory activity. Interestingly, removal of a methyl group (**3t**, IC_{50} = 7.9 nM) also maintained the activity. This SAR information and a co-crystal structure of compound **3f** indicate that a wide variety of small substituents is acceptable on the 4'-position, 5'-position, and 6'-position of the benzene ring; however, contribution of the substituents on these positions may be minimal and given that the nonsubstituted compound **3t** (IC_{50} = 7.9 nM) showed potent nanomolar activity.

With novel and potent CH24H inhibitors developed by our SBDD approach, we then focused on the off-target CYP selectivity of our compounds. Inhibitory activities for CYP3A4,

which is known as a main CYP enzyme for drug metabolism in the liver, were evaluated at a concentration of 10 μM (Table 2). Compared with its potent CH24H inhibition (IC_{50} = 2.7 nM), lead compound **3f** showed good selectivity against CYP3A4 with 67% inhibition at 10 μM. However, a greater degree of selectivity against CYP3A4 was desired to develop these compounds as clinical drug candidates to avoid drug−drug interaction (DDI) risk in humans.

Comparison of CYP3A4 inhibitory activity of compound **3k** (60%) with compound **3f** (67%) indicates that the introduction of the methyl group at the 2-position of the pyridine ring does not affect the CYP3A4 inhibitory activity in stark contrast to the SAR in CH24H (Table 2). This observation suggests that this series of CH24H inhibitors does not bind CYP3A4 with heme ligation, but binds by some nonspecific hydrophobic interactions without heme ligation. In addition, we observed a tendency of reduced CYP3A4 inhibitory activities for compounds **3q−t** in correlation with their lower lipophilicity ($c \log P$) while these compounds maintain CH24H inhibitory activity regardless of their lipophilicity. These results suggest that the binding of these compounds to CYP3A4 is dominated by nonspecific hydrophobic interactions. This observation led us to reduce the CYP3A4 inhibition by designing less lipophilic compounds while maintaining the key interactions necessary for CH24H binding. Based on this strategy to reduce the lipophilicity of the compounds, we continued to optimize compound **3t**, which showed the lowest CYP3A4 inhibitory activity.

Lead Optimization to Improve CYP Selectivity. To reduce the lipophilicity of the molecule, we replaced the benzene and/or pyridine rings of compound **3t** with more polar pyridine or pyrimidine rings (Table 3). Because this design causes only slight changes in the molecular shape, these compounds were expected to maintain the key interaction with Gly369 and heme iron of CH24H. Regarding the positioning of the nitrogen atom on each aryl group, we opted to use the most sterically hindered positions (X^1, X^2, or X^3), which were expected to allow the hydrophobic interaction with the pocket under Helix F and the steroidal cavity to be maintained. Also, by introducing nitrogen at the sterically hindered positions, we could limit the polar surface area value, which is beneficial for better blood−brain barrier (BBB) permeability.

Based on this design, compounds with one additional nitrogen (X^1: **3u**, X^2: **3v**, and X^3: **3w**) and with two additional nitrogens (X^1 and X^2: **3x**, X^2 and X^3: **3y**, X^1 and X^3: **3z**) were synthesized. As we expected, these compounds showed lower lipophilicity ($c \log P$) than lead compound **3t**, as well as improved CYP3A4 inhibitory activities (5−28% inhibition at 10 μM), which were considered low enough to be developed as candidates. Regarding the CH24H inhibitory activity, introduction of one nitrogen at X^1 (**3u**, IC_{50} = 4.3 nM) and X^2 (**3v**, IC_{50} = 7.4 nM) positions maintained the activity. On the other hand, introduction of one nitrogen at the X^3 (**3w**, IC_{50} = 21 nM) position and the introduction of two nitrogens decreased the activity (**3x**: IC_{50} = 19 nM, **3y**: IC_{50} = 100 nM, **3z**: IC_{50} = 36 nM). The clog P values for the compounds **3w−z** (between −0.1 and 0.8) were much lower than that of compound **3t** (2.3), which resulted in lower inhibitory activity not only for CYP3A4 but also for CH24H.

For compounds **3u** and **3v**, which showed potent CH24H inhibitory activity and sufficient CYP3A4 selectivity, we evaluated in vitro metabolic clearance in human hepatic microsomes. The results showed that compound **3v** had

Table 3. CH24H Inhibitory Activities, Lipophilicity ($c \log P$), CYP3A4 Inhibitory Activities, and Human Metabolic Stability of Compounds 3t–z
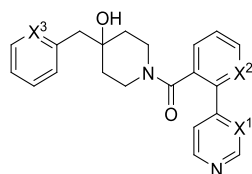
Cpd	X^1	X^2	X^3	$c \log P^d$	CH24H[a] IC_{50} (nM)[b]	CYP3A4 % (10 μM)	clearance[c] μL/(min mg)
3t	CH	CH	CH	2.3	7.9 (2.6–24)	45	120
3u	N	CH	CH	1.5	4.3 (2.8–6.5)	17	70
3v	CH	N	CH	1.4	7.4 (4.8–11)	28	22
3w	CH	CH	N	0.8	21 (14–31)	18	22
3x	N	N	CH	0.6	19 (12–28)	13	17
3y	CH	N	N	−0.1	100 (63–180)	5.3	ND[e]
3z	N	CH	N	0.0	36 (23–60)	8.8	9

[a]Human enzyme. [b]IC_{50} values and 95% confidence intervals (given in parentheses) were calculated from duplicate measurements using a four-parameter logistic curve using XLfit software (IDBS, London, UK). [c]In vitro metabolic clearance in human hepatic microsomes. [d]Calculated log P values were obtained using Daylight.[31] [e]Not determined.

superior metabolic stability (22 μL/(min mg)) and therefore was selected for further characterization including detailed CYP selectivity studies and a PK/PD study in mice.

Co-crystal structure of compound **3v** was obtained and it was confirmed that compound **3v** makes multiple binding interactions with CH24H, in a manner analogous to the binding mode obtained with the lead compound **3f** (Figure 5).
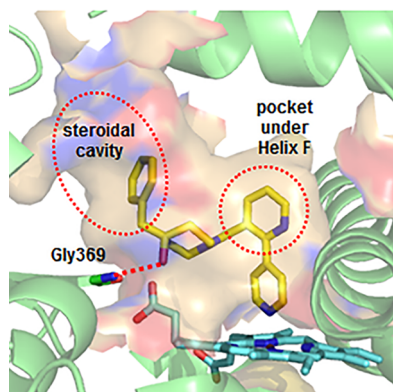
Figure 5. X-ray co-crystal structure of **3v** with CH24H (PDB ID 7LRL).

The inhibitory activities (IC_{50}) of compound **3v** for off-target CYPs were evaluated (Table 4). Compared with the potent CH24H inhibitory activity (IC_{50} = 7.4 nM), compound **3v** showed negligible inhibition not only for CYP3A4 (IC_{50} =

Table 4. Inhibitory Activity (IC_{50}) of Compound 3v for Other CYPs

CYP	IC_{50} (nM)
2C8	62 000
2C9	19 000
2D6	>100 000
3A4	66 000
1A2	>100 000
2C19	14 000

66 000 nM), but also for other CYP enzymes related to drug metabolism (2C8, 2C9, 2D6, 1A2, 2C19). To verify the absence of inhibitory effects of hormone synthesis, several key steroid hormones, such as cortisol, testosterone, aldosterone, and corticosterone, were analyzed in the adrenocortical H295R cell line.[32,33] Ketoconazole, known as a CYP3A4/5 inhibitor, inhibited the entire pathway, whereas **3v** did not show any inhibitory activity on the hormone synthesis in cells (Table 5). As a result, we selected compound **3v** (IC_{50} = 7.4 nM) as a potent and highly selective CH24H inhibitor.

Table 5. Steroidogenic Disruption in H295R Cells

hormone	3v % inhibition (10 μM) (SE)	ketoconazole IC_{50} (μM) (95% CI)
testosterone	−0.4 (9.5)	0.34 (0.30–0.39)
corticosterone	−6.0 (5.0)	2.5 (2.3–2.7)
cortisol	0.2 (7.3)	0.44 (0.39–0.49)
aldosterone	−3.8 (10.7)	1.4 (1.0–2.2)

Effect of Compound 3v on Reducing Brain 24HC Levels. The effect of compound **3v** on the reduction of 24HC concentrations was evaluated in the mouse brain (1, 3, and 10 mg/kg, po). The 24HC levels in the brain as well as the brain concentrations of compound **3v** after oral administration to mice are illustrated in Figure 6. Compound **3v** showed adequate brain exposure for CH24H inhibition, and a dose-dependent concentration of compound **3v** was observed in the brain. Consistent with the brain concentration, compound **3v** showed dose-dependent reduction in 24HC levels in the brain and exhibited significant reduction at 24 h after single-dose administration (33% reduction at 10 mg/kg and 25% reduction at 3 mg/kg from control level, po). This result has demonstrated that compound **3v** is a promising CH24H inhibitory agent with dose-dependent 24HC reduction in the brain.

■ CONCLUSIONS

Here, we report on the design and synthesis of a novel, potent and selective CH24H inhibitor **3v** (IC_{50} = 7.4 nM) starting
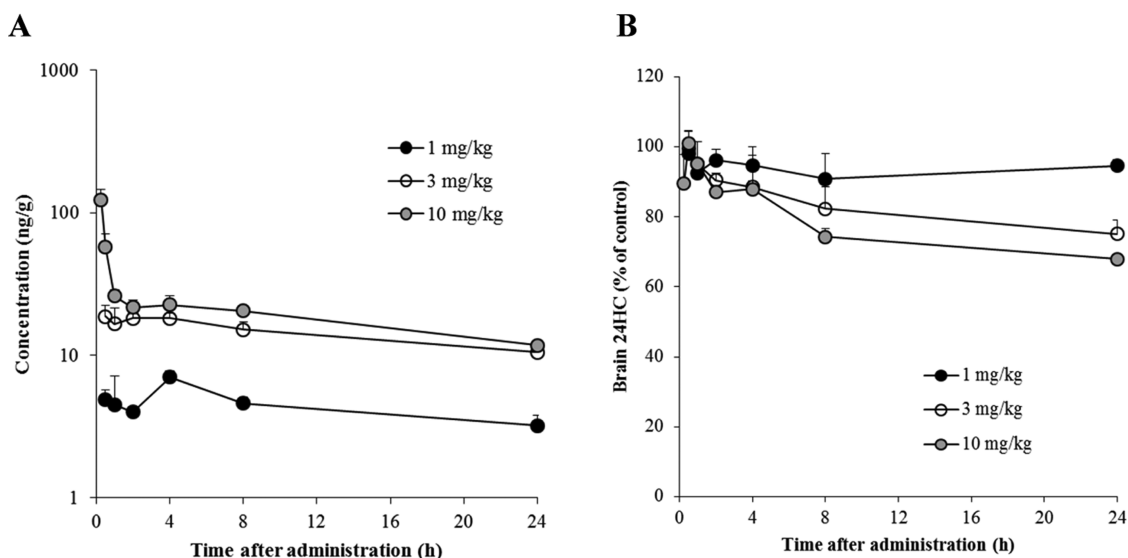
Figure 6. PK/PD study in C57BL/6N mice (7−8 weeks). Brain concentration of (A) **3v** and (B) 24HC level (% control) in mouse brain after oral administration of **3v** at 1, 3, and 10 mg/kg, po. Black (1 mg/kg), white (3 mg/kg), and gray (10 mg/kg) circles represent mean + SD (n = 3).

from a hit derivative **1b** (IC$_{50}$ = 60 nM) by an SBDD approach. Compound **3v** exhibited potent and selective inhibition through four key interactions with CH24H. These interactions include direct ligation to the heme iron by a pyridine nitrogen, hydrophobic interaction with the pocket under Helix F by a pyridine ring, hydrophobic interaction with the steroidal cavity by a benzyl group, and a hydrogen bond between Gly369 and a hydroxyl group. In addition to these specific interactions to CH24H, CYP selectivity of **3v** has been achieved by the adjustment of the lipophilicity of the molecule. Single oral administration of compound **3v** (1, 3, and 10 mg/kg) to mice exhibited a dose-dependent reduction in 24HC levels in the mouse brain, proving that it is brain penetrable. Compound **3v** (soticlestat) is currently under clinical investigation for the treatment of Dravet syndrome and Lennox-Gastaut syndrome.

■ EXPERIMENTAL SECTION

General. All commercially available reagents and solvents were used without further purification. Yields were not optimized. All reactions were monitored by thin-layer chromatography (TLC) analysis on Merck Kieselgel 60 F254 plates or Fuji Silysia NH plates, or liquid chromatography−mass spectrometry (LC−MS) analysis. Microwave-assisted reactions were carried out in a single-mode reactor, Biotage Initiator 2.0 or 2.5 microwave synthesizer. Proton Nuclear Magnetic Resonance (¹H NMR) spectra were recorded on Varian Mercury-300 (300 MHz), Varian (400 MHz), Bruker DPX300 (300 MHz), Bruker Avance III (300 MHz), or Bruker Advance III plus (400 MHz) spectrometer. Chemical shifts are given in parts per million (ppm) downfield from tetramethylsilane (δ) as the internal standard in deuterated solvent, and coupling constants (J) are in hertz (Hz). Data are reported as follows: chemical shift, integration, multiplicity (s = singlet, d = doublet, t = triplet, q = quartet, quint = quintet, m = multiplet, dd = doublet of doublets, td = triplet of doublets, and brs = broad signal), and coupling constants. Analytical TLC was performed on silica gel 60 F$_{254}$ plates (Merck) or NH TLC plates (Fuji Silysia Chemical Ltd.). Extraction by organic solvent was monitored by TLC. Chromatographic purification was performed on silica gel columns [(Merck Kieselgel 60, 70-230 mesh size or 230−400 mesh size, Merck) or (Chromatorex NH-DM 1020, 100−200 mesh size)] or on Purif-Pack (SI or NH, Shoko Scientific). Melting points were determined on a Büchi melting point apparatus B-545. LC−MS analysis was performed on Shimadzu UFLC/MS (Prom-

inence UFLC high-pressure gradient system/LCMS-2020) or Agilent LC/MS system (Agilent 1200SL/Agilent 6130MS), operating in ESI (+ or −) or APCI (+ or −) ionization mode. Analytes were eluted using a linear gradient of 0.05% TFA containing water/acetonitrile or 5 mM ammonium acetate containing water/acetonitrile mobile phase and detected at 220 nm. Preparative HPLC was performed by an automated HPLC system or MS-trigger using ODS column with 10−100% gradient water−acetonitrile containing 0.1% TFA. Elemental analyses were carried out by Takeda Analytical Laboratories, and the results were within ±0.4% of theoretical values. ¹H NMR spectra were in all cases consistent with the proposed structures. The purities of all tested compounds in biological systems were confirmed to be more than 95% pure as determined by analytical HPLC.

Methyl 5-Methyl-2-(pyridine-4-yl)benzoate (2a). To a mixture of methyl 2-bromo-5-methylbenzoate **4a** (712 mg, 3.11 mmol), DME (15.0 mL), and water (3.00 mL) were added pyridine-4-boronic acid **5a** (573 mg, 4.66 mmol), sodium carbonate (659 mg, 6.22 mmol), and Pd(PPh$_3$)$_4$ (180 mg, 0.16 mmol) at room temperature. The mixture was refluxed under N$_2$ overnight. The reaction mixture was diluted with ethyl acetate (EtOAc), filtered with silica pad, and concentrated in vacuo. The residue was purified by column chromatography (silica gel, 30−50% EtOAc/hexane) to give **2a** (548 mg, 2.41 mmol, 78%) as a colorless oil. ¹H NMR (CDCl$_3$) δ 2.44 (3H, s), 3.65 (3H, s), 7.22 (3H, dd, J = 6.6, 4.7 Hz), 7.39 (1H, d, J = 8.3 Hz), 7.73 (1H, s), 8.61 (2H, d, J = 6.0 Hz); MS (ESI) m/z: 228 (M + H)$^+$.

Methyl 5-Chloro-2-(pyridin-4-yl)benzoate (2b). Compound **2b** (1.46 g, 5.89 mmol, 49%) was obtained as a colorless oil by a method similar to that described for **2a**. ¹H NMR (CDCl$_3$) δ 3.68 (3H, s), 7.17−7.30 (3H, m), 7.55 (1H, dd, J = 8.2, 2.2 Hz), 7.91 (1H, d, J = 2.2 Hz), 8.61−8.67 (2H, m); MS (ESI) m/z: 248 (M + H)$^+$.

Methyl 5-Methoxy-2-(pyridin-4-yl)benzoate (2c). A mixture of methyl 2-bromo-5-methoxybenzoate **4c** (3.00 g, 12.2 mmol), Pd(PPh$_3$)$_4$ (0.707 g, 0.610 mmol), sodium carbonate (2.59 g, 24.5 mmol), pyridine-4-boronic acid **5a** (1.81 g, 14.7 mmol), DME (16.0 mL), and water (4.0 mL) was heated at 140 °C for 1 h under microwave irradiation. The mixture was quenched with water at room temperature and extracted with EtOAc. The organic layer was separated, washed with brine, dried over Na$_2$SO$_4$, and concentrated in vacuo. The residue was purified by column chromatography (NH silica gel, 5−20% EtOAc/hexane) to give **2c** (1.14 g, 4.69 mmol, 38%) as a pale yellow oil. ¹H NMR (CDCl$_3$) δ 3.66 (3H, s), 3.89 (3H, s), 7.11 (1H, dd, J = 8.3, 2.6 Hz), 7.16−7.22 (2H, m), 7.23−7.30 (1H, m), 7.42 (1H, d, J = 2.6 Hz), 8.56−8.63 (2H, m); MS (ESI) m/z: 244 (M + H)$^+$.

Methyl 5-Fluoro-2-(pyridin-4-yl)benzoate (2d). Compound **2d** (1.08 g, 4.65 mmol, 30%) was obtained as a white solid by a method similar to that described for **2c**. ^{1}H NMR (CDCl$_3$) δ 3.69 (3H, s), 7.16−7.26 (2H, m), 7.31 (2H, ddt, J = 7.1, 3.7, 1.6 Hz), 7.55−7.74 (1H, m), 8.44−8.85 (2H, m).

Ethyl 2-(Pyridin-4-yl)benzoate (2e). Compound **2e** (2.84 g, 12.5 mmol, 48%) was obtained as a white solid by a method similar to that described for **2c**. ^{1}H NMR (CDCl$_3$) δ 1.04 (3H, t, J = 7.2 Hz), 4.12 (2H, q, J = 7.2 Hz), 7.18−7.26 (2H, m), 7.32 (1H, dd, J = 7.5, 1.1 Hz), 7.44−7.53 (1H, m), 7.53−7.63 (1H, m), 7.93 (1H, dd, J = 7.5, 1.1 Hz), 8.59−8.66 (2H, m); MS (ESI) m/z: 228 (M + H)$^+$.

5-Methyl-2-(pyridin-4-yl)benzoic Acid Hydrochloride (2f). A mixture of **2a** (8.81 g, 38.8 mmol), 6 M HCl (64.6 mL, 388 mmol), and AcOH (100 mL) was refluxed for 5 h. The solvent was removed in vacuo, and the obtained precipitate was washed with EtOAc and filtered to give **2f** (6.55 g, 26.2 mmol, 68%) as a white solid. ^{1}H NMR (DMSO-d_6) δ 2.44 (3H, s), 7.38 (1H, d, J = 7.9 Hz), 7.55 (1H, d, J = 7.9 Hz), 7.82 (1H, s), 7.90 (2H, brs), 8.78−8.95 (2H, m); MS (ESI) m/z: 214 (M + H)$^+$−(HCl).

5-Chloro-2-(pyridin-4-yl)benzoic Acid Hydrochloride (2g). Compound **2g** (1.36 g, 5.03 mmol, 86%) was obtained as a white solid by a method similar to that described for **2f**. ^{1}H NMR (DMSO-d_6) δ 7.51 (1H, d, J = 8.2 Hz), 7.83 (1H, dd, J = 8.2, 2.2 Hz), 7.98 (3H, s), 8.74−9.09 (2H, m).

5-Methoxy-2-(pyridin-4-yl)benzoic Acid Hydrochloride (2h). Compound **2h** (1.19 g, 4.48 mmol, 96%) was obtained as a white solid by a method similar to that described for **2f**. ^{1}H NMR (DMSO-d_6) δ 3.90 (3H, s), 7.17−7.37 (1H, m), 7.41−7.54 (2H, m), 7.83−8.02 (2H, m), 8.76−8.98 (2H, m).

5-Fluoro-2-(pyridin-4-yl)benzoic Acid Hydrochloride (2i). Compound **2i** (1.10 g, 4.34 mmol, 95%) was obtained as a pale yellow solid by a method similar to that described for **2f**. ^{1}H NMR (DMSO-d_6) δ 7.46−7.69 (2H, m), 7.79 (1H, d, J = 2.7 Hz), 7.99 (2H, d, J = 6.6 Hz), 8.84−8.99 (2H, m).

2-(Pyridin-4-yl)benzoic Acid Hydrochloride (2j). Compound **2j** (3.62 g, 15.4 mmol, 76%) was obtained as a white solid by a method similar to that described for **2f**. ^{1}H NMR (DMSO-d_6) δ 7.49 (1H, dd, J = 7.6, 1.1 Hz), 7.62−7.84 (2H, m), 7.94−8.12 (3H, m), 8.82−9.04 (2H, m); MS (ESI) m/z: 200 (M + H)$^+$−(HCl).

Methyl 2-(4,4,5,5-Tetramethyl-1,3,2-dioxaborolan-2-yl)benzoate (6). A mixture of methyl 2-bromobenzoate **4f** (5.30 g, 24.7 mmol), bis(pinacolato)diboron (9.39 g, 37.0 mmol), Pd(dppf)Cl$_2$·CH$_2$Cl$_2$ (1.01 g, 1.23 mmol), and potassium acetate (7.26 g, 73.9 mmol) in a mixture of THF (100 mL) and DMSO (5.00 mL) was stirred at 80 °C under Ar for 5 h. The mixture was poured into water and extracted with EtOAc. The organic layer was dried over MgSO$_4$, filtered, and concentrated in vacuo. The residue was purified by column chromatography (silica gel, 1−10% EtOAc/hexane) to give **6** (6.30 g, 24.0 mmol, 98%) as a colorless oil. ^{1}H NMR (CDCl$_3$) δ 1.42 (12H, s), 3.91 (3H, s), 7.36−7.46 (1H, m), 7.47−7.55 (2H, m), 7.94 (1H, d, J = 7.6 Hz).

Methyl 2-(6-Chloropyrimidin-4-yl)benzoate (7). A mixture of **6** (2.00 g, 7.63 mmol), 4,6-dichloropyrimidine (1.36 g, 9.16 mmol), Pd(PPh$_3$)$_4$ (0.441 g, 0.380 mmol), and sodium carbonate (2.43 g, 22.9 mmol) in DME (10.0 mL) and water (2.00 mL) was stirred at 150 °C under microwave irradiation for 1 h. The mixture was poured into water and extracted with EtOAc. The organic layer was washed with brine, dried over Na$_2$SO$_4$, filtered, and concentrated in vacuo. The residue was purified by column chromatography (silica gel, 3−15% EtOAc/hexane) to give **7** (0.600 g, 2.41 mmol, 32%) as a pale yellow oil. ^{1}H NMR (CDCl$_3$) δ 3.75 (3H, s), 7.49−7.67 (4H, m), 7.90 (1H, dd, J = 7.3, 1.3 Hz), 9.01 (1H, d, J = 1.3 Hz).

2-(Pyrimidin-4-yl)benzoic Acid Hydrochloride (2k). A mixture of **7** (0.600 g, 2.41 mmol), triethylamine (1.68 mL, 12.1 mmol), and 10% Pd-C (0.257 g, 0.120 mmol) in MeOH (20.0 mL) was hydrogenated under balloon pressure at room temperature for 1 h. The catalyst was removed by filtration and the filtrate was concentrated in vacuo. The mixture was diluted with EtOAc, washed with brine, dried over Na$_2$SO$_4$, filtered, and concentrated in vacuo. A mixture of the residue, AcOH (2.00 mL), and 6 M HCl (10.0 mL,

60.0 mmol) was refluxed for 5 h. The mixture was concentrated in vacuo. The residual solid was washed with EtOAc to give **2k** (0.446 g, 1.89 mmol, 82%) as a beige solid. ^{1}H NMR (DMSO-d_6) δ 7.57−7.71 (3H, m), 7.75 (1H, dd, J = 5.3, 1.5 Hz), 7.78−7.85 (1H, m), 8.87 (1H, d, J = 5.3 Hz), 9.22 (1H, s), 10.59−11.85 (1H, brs).

6-[3-(Methoxycarbonyl)pyridin-2-yl]pyrimidine 1-Oxide (8). A mixture of methyl 2-chloropyridine-3-carboxylate **4g** (1.52 mL, 11.7 mmol), potassium carbonate (3.22 g, 23.3 mmol), pyrimidine N-oxide (3.36 g, 35.0 mmol), copper(I) cyanide (0.104 g, 1.17 mmol), Pd(OAc)$_2$ (0.131 g, 0.580 mmol), and P(t-Bu)$_3$·HBF$_4$ (0.507 g, 1.75 mmol) in dioxane (20.0 mL) was heated to 150 °C under microwave irradiation for 2 h. The mixture was diluted with EtOAc and the precipitate was filtered through celite. The filtrate was concentrated in vacuo. The residue was purified by column chromatography (silica gel, 30−100% EtOAc/hexane) to give **8** (0.480 g, 2.08 mmol, 18%) as a brown solid. ^{1}H NMR (CDCl$_3$) δ 3.87 (3H, s), 7.54 (1H, dd, J = 7.9, 4.9 Hz), 7.71 (1H, dd, J = 4.9, 0.8 Hz), 8.28 (1H, dd, J = 7.9, 1.5 Hz), 8.35 (1H, d, J = 4.9 Hz), 8.85 (1H, dd, J = 4.9, 1.5 Hz), 9.00 (1H, d, J = 0.8 Hz); MS (ESI) m/z: 232 (M + H)$^+$.

2-(Pyrimidin-4-yl)nicotinic Acid Dihydrochloride (2l). Compound **2l** (0.260 g, 0.949 mmol, quant) was obtained as a brown oil by a method similar to that described for **2k**. MS (ESI) m/z: 202 (M + H)$^+$.

(4-Benzylpiperidin-1-yl)(5-methyl-2-(pyridin-4-yl)phenyl)-methanone (3a). A mixture of **2f** (300 mg, 1.20 mmol), 4-benzylpiperidine **9a** (0.232 mL, 1.32 mmol), DMT-MM (399 mg, 1.44 mmol), and DMF (5.00 mL) was stirred at room temperature for 3 h. Additional 4-benzylpiperidine (0.232 mL, 1.32 mmol) was added to this solution. After stirring overnight, the mixture was quenched with saturated aqueous NaHCO$_3$ at room temperature and extracted with EtOAc. The organic layer was separated, washed with brine, dried over Na$_2$SO$_4$, and concentrated in vacuo. The residue was purified by column chromatography (NH silica gel, 30−50% EtOAc/hexane) to give **3a** (287 mg, 0.775 mmol, 65%) as a colorless oil. ^{1}H NMR (CDCl$_3$) δ 0.37−1.04 (1H, m), 1.06−1.67 (3H, m), 2.03−2.76 (8H, m), 3.07−3.27 (1H, m), 4.64 (1H, t, J = 12.4 Hz), 6.92−7.55 (10H, m), 8.52−8.76 (2H, m); ^{13}C NMR (CDCl$_3$) δ 18.43, 21.09, 21.13, 30.92, 31.52, 32.09, 37.60, 37.83, 41.56, 41.86, 42.72, 46.48, 47.06, 58.30, 123.23, 123.82, 125.98, 126.06, 128.17, 128.22, 128.25, 128.27, 128.88, 128.94, 128.99, 130.23, 130.35, 132.49, 132.89, 135.59, 135.85, 139.42, 139.77, 147.55, 147.64, 149.77, 149.82, 169.08, 169.13; MS (ESI) m/z: 371 (M + H)$^+$.

1-Benzyl-4-(5-methyl-2-(pyridin-4-yl)benzoyl)piperazin-2-one (3d). A mixture of **2f** (600 mg, 2.40 mmol), piperazin-2-one (361 mg, 3.60 mmol), HATU (137 mg, 3.60 mmol), triethylamine (1.68 mL, 12.0 mmol), and DMF (6.00 mL) was stirred at room temperature for 3 h. The mixture was poured into water and extracted with EtOAc. The organic layer was washed with brine, dried over Na$_2$SO$_4$, filtered, and concentrated in vacuo. To a mixture of the residual compound, benzyl bromide (0.100 mL, 0.840 mmol), and DMF (2.00 mL) was added NaH (30.5 mg, 0.76 mmol) at room temperature, and the mixture was stirred at the same temperature for 3 h. The mixture was poured into water and extracted with EtOAc. Then the mixture was washed with brine, dried over Na$_2$SO$_4$, and filtered on NH silica gel. The filtrate was concentrated in vacuo. The residue was purified by preparative HPLC. The desired fraction was neutralized with saturated aqueous NaHCO$_3$ and extracted with EtOAc. The organic layer was separated, dried over MgSO$_4$, and concentrated in vacuo to give **3d** (90.0 mg, 0.233 mmol, 10%) as a colorless oil. ^{1}H NMR (CDCl$_3$) δ 2.34−2.48 (3H, m), 2.90−4.67 (8H, m), 7.09−7.16 (2H, m), 7.21−7.40 (8H, m), 8.58−8.63 (2H, m); MS (ESI) m/z: 386 (M + H)$^+$.

(4-Benzyl-3-hydroxypiperidin-1-yl)(5-methyl-2-(pyridin-4-yl)-phenyl)methanone (3e). Compound **3e** (257 mg, 0.665 mmol, 88%) was obtained as a white solid by a method similar to that described for **3a**. ^{1}H NMR (300 MHz, CDCl$_3$) δ 0.31−0.07 (1H, m), 0.56−1.65 (3H, m), 1.78−2.75 (7H, m), 2.81−3.59 (3H, m), 4.39−4.80 (1H, m), 6.94−7.55 (10H, m), 8.52−8.68 (2H, m); MS (ESI) m/z: 387 (M + H)$^+$.

(4-Benzyl-4-hydroxypiperidin-1-yl)(5-methyl-2-(pyridin-4-yl)phenyl)methanone (3f). A mixture of **2f** (330 mg, 1.32 mmol), 4-benzyl-4-hydroxypiperidine **9f** (379 mg, 1.98 mmol), HATU (753 mg, 1.98 mmol), and triethylamine (0.917 mL, 6.60 mmol) in DMF (5.00 mL) was stirred at room temperature overnight. The mixture was quenched with water and extracted with EtOAc. The organic layer was separated, washed with brine, dried over Na_2SO_4, and concentrated in vacuo. The residue was purified by column chromatography (NH silica gel, 50−80% EtOAc/hexane) to give **3f** (401 mg, 1.04 mmol, 79%) as a white solid. ^{1}H NMR ($CDCl_3$) δ 0.03−1.61 (5H, m), 2.26−2.83 (6H, m), 2.87−3.16 (2H, m), 4.34−4.59 (1H, m), 6.93−7.61 (10H, m), 8.50−8.74 (2H, m); MS (ESI) m/z: 387 (M + H)[+].

(4-Hydroxypiperidin-1-yl)(5-methyl-2-(pyridin-4-yl)phenyl)-methanone (3h). Compound **3h** (112 mg, 0.378 mmol, 32%) was obtained as a colorless oil by a method similar to that described for **3a**. ^{1}H NMR ($CDCl_3$) δ 0.54−1.31 (2H, m), 1.40−1.81 (2H, m), 2.42 (3H, s), 2.46−2.91 (1H, m), 2.95−3.35 (2H, m), 3.71 (1H, dd, J = 7.9, 4.2 Hz), 3.93−4.08 (1H, m), 7.22 (1H, d, J = 7.9 Hz), 7.28−7.36 (2H, m), 7.41 (2H, t, J = 5.7 Hz), 8.57−8.66 (2H, m); MS (ESI) m/z: 297 (M + H)[+].

(4-Ethyl-4-hydroxypiperidin-1-yl)(5-methyl-2-(pyridin-4-yl)-phenyl)methanone (3i). Compound **3i** (197 mg, 0.607 mmol, 36%) was obtained as a colorless oil by a method similar to that described for **3f**. ^{1}H NMR ($CDCl_3$) δ 0.12−1.63 (10H, m), 2.41 (3H, s), 2.58−3.20 (3H, m), 4.30−4.49 (1H, m), 7.13−7.53 (5H, m), 8.60 (2H, d, J = 4.5 Hz); ^{13}C NMR ($CDCl_3$) δ 6.99, 15.24, 21.10, 34.97, 35.44, 35.56, 35.64, 35.92, 36.35, 37.51, 42.58, 42.98, 65.82, 69.29, 69.41, 123.26, 123.69, 128.00, 128.25, 128.89, 129.02, 130.25, 130.35, 132.30, 135.78, 139.38, 139.53, 147.61, 149.71, 168.97; MS (ESI) m/z: 325 (M + H)[+].

(4-Benzyl-4-hydroxypiperidin-1-yl)(5-chloro-2-(pyridin-4-yl)-phenyl)methanone (3q). Compound **3q** (228 mg, 0.560 mmol, 76%) was obtained as a white solid by a method similar to that described for **3f**. ^{1}H NMR (300 MHz, $CDCl_3$), ^{1}H NMR ($CDCl_3$) δ 0.97−1.74 (5H, m), 2.43 (1H, d, J = 5.7 Hz), 2.57−3.18 (4H, m), 4.44 (1H, t, J = 13.8 Hz), 6.99−7.18 (2H, m), 7.22−7.55 (8H, m), 8.57−8.78 (2H, m); ^{13}C NMR ($CDCl_3$) δ 36.28, 37.51, 37.58, 38.62, 42.49, 42.93, 49.06, 49.14, 68.79, 69.09, 123.06, 123.67, 126.94, 127.59, 127.89, 128.46, 129.70, 129.79, 130.33, 130.42, 130.50, 133.65, 134.33, 135.43, 135.46, 135.58, 137.09, 137.36, 146.40, 146.49, 149.93, 150.02, 167.20, 167.27; MS (ESI) m/z: 407 (M + H)[+].

(4-Benzyl-4-hydroxypiperidin-1-yl)(5-methoxy-2-(pyridin-4-yl)phenyl)methanone (3r). Compound **3r** (156 mg, 0.388 mmol, 34%) was obtained as a white solid by a method similar to that described for **3f**. ^{1}H NMR ($CDCl_3$) δ 0.05−1.63 (5H, m), 2.31−2.84 (3H, m), 2.89−3.16 (2H, m), 3.79−3.93 (3H, m), 4.34−4.58 (1H, m), 6.83−7.15 (4H, m), 7.18−7.53 (6H, m), 8.48−8.74 (2H, m); ^{13}C NMR ($CDCl_3$) δ 35.76, 36.22, 36.30, 36.88, 37.44, 37.50, 42.39, 42.86, 49.05, 49.18, 55.54, 68.86, 69.14, 112.66, 112.69, 115.53, 115.75, 123.10, 123.71, 126.87, 126.90, 127.50, 128.24, 128.42, 130.35, 130.39, 130.42, 130.52, 135.56, 135.71, 136.79, 137.12, 147.22, 147.33, 149.75, 149.84, 160.24, 160.35, 168.55, 168.61; MS (ESI) m/z: 403 (M + H)[+].

(4-Benzyl-4-hydroxypiperidin-1-yl)(5-fluoro-2-(pyridin-4-yl)-phenyl)methanone (3s). Compound **3s** (147 mg, 0.376 mmol, 64%) was obtained as a white solid by a method similar to that described for **3f**. ^{1}H NMR ($CDCl_3$) δ 0.78−1.72 (5H, m), 2.33−2.51 (1H, m), 2.55−2.81 (2H, m), 2.87−3.21 (2H, m), 4.44 (1H, brs), 6.95−7.35 (8H, m), 7.36−7.58 (2H, m), 8.48−8.77 (2H, m); ^{13}C NMR ($CDCl_3$) δ 35.73, 36.28, 37.53, 42.86, 49.06, 49.17, 68.79, 114.86, 123.17, 123.77, 126.95, 128.47, 130.34, 131.12, 149.98, 167.28; MS (ESI) m/z: 391 (M + H)[+].

(4-Benzyl-4-hydroxypiperidin-1-yl)(2-(pyrimidin-4-yl)phenyl)-methanone (3u). Compound **3u** (110 mg, 0.295 mmol, 35%) was obtained as a yellow oil by a method similar to that described for **3f**. ^{1}H NMR ($CDCl_3$) δ 1.29−1.42 (2H, m), 1.50−1.78 (3H, m), 2.61−2.82 (2H, m), 2.86−3.40 (3H, m), 4.37−4.60 (1H, m), 7.06−7.46 (6H, m), 7.47−7.84 (4H, m), 8.66−8.81 (1H, m), 8.85−9.27 (1H, m); ^{13}C NMR ($CDCl_3$) δ 35.89, 36.12, 37.58, 43.47, 69.49, 69.60,

119.97, 127.00, 127.45, 128.51, 129.33, 129.37, 130.47, 135.74, 157.27, 158.38; MS (ESI) m/z: 374 (M + H)[+].

(4-Hydroxy-4-(pyridin-2-ylmethyl)piperidin-1-yl)(2-(pyridin-4-yl)phenyl)methanone (3w). Compound **3w** (143 mg, 0.383 mmol, 40%) was obtained as a colorless oil by a method similar to that described for **3e**. ^{1}H NMR ($CDCl_3$) δ 0.02−1.57 (5H, m), 2.54 (1H, s), 2.76−3.32 (4H, m), 4.42 (1H, d, J = 11.0 Hz), 6.98−7.10 (1H, m), 7.10−7.20 (1H, m), 7.31−7.55 (6H, m), 7.62 (1H, t, J = 7.6 Hz), 8.42 (1H, d, J = 4.9 Hz), 8.57−8.72 (2H, m); ^{13}C NMR ($CDCl_3$) δ 35.97, 36.79, 36.92, 37.56, 42.59, 42.86, 47.14, 47.44, 69.17, 69.48, 77.27, 121.72, 123.21, 123.95, 124.50, 127.31, 127.75, 128.86, 129.00, 129.17, 129.31, 129.42, 135.05, 136.09, 137.06, 147.70, 148.23, 148.36, 149.86, 158.64, 168.74; MS (ESI) m/z: 374 (M + H)[+].

(4-Benzyl-4-hydroxypiperidin-1-yl)(2-(pyrimidin-4-yl)pyridin-3-yl)methanone (3x). Compound **3x** (85.0 mg, 0.227 mmol, 26%) was obtained as a pale yellow solid by a method similar to that described for **3f**. ^{1}H NMR ($CDCl_3$) δ 1.27−2.00 (5H, m), 2.80 (2H, s), 3.09−3.52 (3H, m), 4.43−4.67 (1H, m), 7.12−7.22 (2H, m), 7.28−7.50 (4H, m), 7.61−7.75 (1H, m), 8.16−8.27 (1H, m), 8.73−9.23 (3H, m); ^{13}C NMR ($CDCl_3$) δ 35.65, 35.84, 36.19, 36.48, 37.56, 37.77, 42.84, 43.68, 49.29, 50.06, 69.43, 69.94, 118.99, 119.36, 124.64, 124.90, 127.03, 128.53, 130.52, 132.93, 133.12, 135.76, 135.90, 149.52, 150.49, 151.11, 157.56, 157.91, 158.22, 162.58, 162.85, 168.07, 169.14, 189.88, 190.53, 193.28; MS (ESI) m/z: 375 (M + H)[+].

(4-Hydroxy-4-(pyridin-2-ylmethyl)piperidin-1-yl)(2-(pyrimidin-4-yl)phenyl)methanone (3z). Compound **3z** (85.0 mg, 0.227 mmol, 26%) was obtained as a pale yellow solid by a method similar to that described for **3f**. ^{1}H NMR ($CDCl_3$) δ 1.30−1.81 (4H, m), 2.68−3.46 (5H, m), 4.43 (1H, d, J = 13.2 Hz), 6.06 (1H, brs), 7.09 (1H, d, J = 7.6 Hz), 7.13−7.20 (1H, m), 7.36−7.42 (1H, m), 7.47−7.56 (2H, m), 7.58−7.80 (3H, m), 8.46 (1H, d, J = 4.2 Hz), 8.76 (1H, brs), 9.25 (1H, d, J = 1.1 Hz); ^{13}C NMR ($CDCl_3$) δ 121.77, 124.50, 127.37, 127.50, 129.27, 129.32, 130.47, 134.90, 136.81, 137.07, 148.36, 157.22, 158.46, 158.68, 158.80, 169.20; MS (ESI) m/z: 375 (M + H)[+].

(4-Benzyl-4-hydroxypiperidin-1-yl)(2-bromo-5-methylphenyl)-methanone (10a). A mixture of 2-bromo-5-methylbenzoic acid **4h** (3.00 g, 14.0 mmol), HATU (6.37 g, 16.7 mmol), 4-benzylpiperidin-4-ol (2.94 g, 15.4 mmol), triethylamine (9.72 mL, 69.8 mmol), and DMF (50.0 mL) was stirred at room temperature for 5 h. The mixture was quenched with water at room temperature and extracted with EtOAc. The organic layer was separated, washed with brine, dried over Na_2SO_4, and concentrated in vacuo. The residue was purified by column chromatography (NH silica gel, 50−80% EtOAc/Hexane) to give **10a** (4.51 g, 11.6 mmol, 83%) as a white solid. ^{1}H NMR ($CDCl_3$) δ 1.22−1.97 (5H, m), 2.31 (3H, d, J = 7.5 Hz), 2.79 (2H, s), 3.07−3.54 (3H, m), 4.54 (1H, t, J = 11.9 Hz), 6.96−7.23 (4H, m), 7.28−7.50 (4H, m); MS (ESI) m/z: 388, 390 (M, M + 2H)[+].

(4-Benzyl-4-hydroxypiperidin-1-yl)(2-chloropyridin-3-yl)-methanone (10h). To a mixture of 2-chloronicotinic acid **4m** (1.00 g, 6.35 mmol), toluene (15 mL), and DME (5 mL) was added thionyl chloride (0.505 mL, 6.92 mmol), and the mixture was stirred at 90 °C under N_2 for 4 h. The reaction mixture was concentrated under reduced pressure. The residue was dissolved in THF (15 mL); then, triethylamine (0.965 mL, 6.92 mmol) and 4-benzyl-4-hydroxypiperidine **9f** (1.10 g, 5.77 mmol) were added and the reaction mixture was stirred at room temperature under N_2 overnight. To the reaction mixture, saturated aqueous $NaHCO_3$ was added and extracted with EtOAc. The organic layer was separated, washed with brine, dried over Na_2SO_4, and concentrated in vacuo. The residue was purified by column chromatography (silica gel, 50−100% EtOAc/hexane) to give **10h** (1.86 g, 5.62 mmol, 97%) as a white solid. ^{1}H NMR ($CDCl_3$) δ 1.22−1.94 (5H, m), 2.80 (2H, d, J = 5.3 Hz), 3.08−3.60 (3H, m), 4.47−4.66 (1H, m), 7.14−7.23 (2H, m), 7.27−7.40 (4H, m), 7.55−7.71 (1H, m), 8.43 (1H, dd, J = 4.5, 1.9 Hz); MS (ESI) m/z: 331 (M + H)[+].

(4-Benzyl-4-methoxypiperidin-1-yl)(5-methyl-2-(pyridin-4-yl)-phenyl)methanone (3g). To a solution of **10a** (314 mg, 0.810 mmol) in DMF (5.00 mL) was added sodium hydride (52.9 mg, 1.21 mmol)

at 0 °C and stirred for 30 min at the same temperature. Iodomethane (0.252 mL, 4.04 mmol) was added to this solution at 0 °C, and the reaction mixture was stirred at room temperature overnight. The mixture was quenched with water at 0 °C and extracted with EtOAc. The organic layer was separated, washed with brine, dried over Na$_2$SO$_4$, and concentrated in vacuo. The resulting crude compound (**10b**), Pd(PPh$_3$)$_4$ (46.8 mg, 0.0400 mmol), sodium carbonate (172 mg, 1.62 mmol), pyridine-4-boronic acid **5a** (110 mg, 0.890 mmol), DME (5.00 mL), and water (1.00 mL) was heated at 140 °C for 1 h under microwave irradiation. The mixture was quenched with water at room temperature and extracted with EtOAc. The organic layer was separated, washed with brine, dried over Na$_2$SO$_4$, and concentrated in vacuo. The residue was purified by column chromatography (NH silica gel, 50−80% EtOAc/hexane) to give **3g** (231 mg, 0.577 mmol, 71%) as a colorless oil. ^{1}H NMR (CDCl$_3$) δ 1.23−1.45 (1H, m), 1.57 (5H, s), 2.29−2.49 (1H, m), 2.66−2.93 (2H, m), 3.68 (2H, s), 3.79 (3H, s), 3.89 (1H, d, J = 14.0 Hz), 4.74 (1H, d, J = 13.2 Hz), 6.78−6.91 (2H, m), 7.10−7.31 (7H, m), 7.33−7.45 (1H, m), 8.60−8.68 (2H, m); ^{13}C NMR (CDCl$_3$) δ 21.08, 32.05, 32.28, 33.56, 33.94, 37.17, 37.24, 41.56, 42.06, 42.17, 42.68, 48.64, 48.68, 73.54, 73.77, 123.15, 123.67, 126.40, 126.45, 128.03, 128.09, 128.28, 128.87, 128.96, 130.05, 130.19, 130.22, 130.32, 132.44, 133.03, 135.48, 135.76, 136.28, 136.48, 139.32, 139.44, 147.44, 147.49, 149.90, 168.94, 169.03; MS (ESI) m/z: 401 (M + H)$^+$.

(4-Hydroxy-4-phenylpiperidin-1-yl)(5-methyl-2-(pyridin-4-yl)-phenyl)methanone (3j). A mixture of 2-bromo-5-methylbenzoic acid **4h** (100 mg, 0.470 mmol), HATU (265 mg, 0.700 mmol), 4-hydroxy-4-phenylpiperidine **9j** (99.0 mg, 0.560 mmol), triethylamine (0.129 mL, 0.930 mmol), and DMF (3.00 mL) was stirred at room temperature for 3 h. The mixture was quenched with water at room temperature and extracted with EtOAc. The organic layer was separated, washed with water and brine, dried over Na$_2$SO$_4$, and concentrated in vacuo. The resulting crude compound, Pd(PPh$_3$)$_4$ (27.2 mg, 0.0200 mmol), 2 M aqueous solution of sodium carbonate (0.470 mL, 0.940 mmol), pyridine-4-boronic acid **5a** (87.0 mg, 0.710 mmol), and DME (5.00 mL) were heated at 120 °C under microwave irradiation for 1 h. The mixture was quenched with water at room temperature and extracted with EtOAc. The organic layer was separated, washed with brine, dried over Na$_2$SO$_4$, and concentrated in vacuo. The residue was purified by column chromatography (silica gel, 50−100% EtOAc/hexane), followed by crystallization (EtOAc/hexane) to give **3j** (112 mg, 0.301 mmol, 64%) as a white solid. Mp 188 °C (EtOAc/hexane); ^{1}H NMR (CDCl$_3$) δ 0.66−2.17 (5H, m), 2.43 (3H, s), 2.69−3.40 (3H, m), 4.46−4.76 (1H, m), 7.05 (1H, d, J = 7.4 Hz), 7.19−7.45 (9H, m), 7.52 (1H, d, J = 6.0 Hz), 8.57−8.74 (1H, m); ^{13}C NMR (CDCl$_3$) δ 21.12, 37.38, 37.56, 37.61, 37.68, 38.00, 38.64, 42.70, 43.24, 71.04, 71.08, 123.26, 123.81, 124.03, 124.39, 127.15, 127.34, 128.03, 128.24, 128.45, 129.04, 130.31, 130.45, 132.36, 133.03, 135.40, 135.72, 139.46, 139.58, 147.47, 147.61, 147.66, 149.67, 149.87, 169.09; MS (ESI) m/z: 373 (M + H)$^+$.

(4-Benzyl-4-hydroxypiperidin-1-yl)(5-methyl-2-(2-methylpyridin-4-yl)phenyl)methanone (3k). A mixture of **10a** (100 mg, 0.260 mmol), (2-methylpyridin-4-yl)boronic acid **5b** (52.9 mg, 0.390 mmol), 3 M aqueous solution of potassium carbonate (0.172 mL, 0.520 mmol), Pd(PPh$_3$)$_4$ (14.9 mg, 0.0100 mmol), and DME (1.00 mL) was heated at 120 °C for 1 h under microwave irradiation. The mixture was poured into water at room temperature and extracted with EtOAc. The organic layer was separated, washed with brine, dried over MgSO$_4$, and concentrated in vacuo. The residue was purified by column chromatography (NH silica gel, 50−100% EtOAc/hexane) to give **3k** (26.7 mg, 0.0670 mmol, 26%) as a colorless oil. ^{1}H NMR (CDCl$_3$) δ 1.14−1.72 (6H, m), 2.31−2.51 (4H, m), 2.55−2.82 (4H, m), 2.88−3.16 (2H, m), 4.36−4.60 (1H, m), 7.04 (1H, d, J = 6.1 Hz), 7.14 (1H, d, J = 8.0 Hz), 7.18−7.41 (8H, m), 8.41−8.61 (1H, m); ^{13}C NMR (CDCl$_3$) δ 21.09, 24.46, 24.57, 35.93, 36.12, 36.38, 36.88, 37.36, 37.43, 42.43, 42.84, 49.17, 68.91, 69.19, 120.34, 120.99, 122.58, 123.20, 126.86, 128.04, 128.40, 128.80, 128.99, 130.32, 132.59, 133.31, 135.42, 135.59, 135.71,

139.15, 139.33, 147.79, 147.91, 149.09, 149.25, 158.55, 168.99, 169.10; MS (ESI) m/z: 401 (M + H)$^+$.

(4-Benzyl-4-hydroxypiperidin-1-yl)(2-(3-fluoropyridin-4-yl)-5-methylphenyl)methanone (3l). A mixture of **10a** (50.0 mg, 0.130 mmol), 2 M aqueous solution of sodium carbonate (0.193 mL, 0.390 mmol), 3-fluoropyridin-4-ylboronic acid **5c** (36.3 mg, 0.260 mmol), Pd(dppf)Cl$_2$·CH$_2$Cl$_2$ (10.5 mg, 0.0100 mmol), and diglyme (2.00 mL) was heated at 120 °C for 5 h under microwave irradiation. The mixture was diluted with EtOAc, silica powder was added to this suspension at 0 °C, and the resulting mixture was stirred at the same temperature for 10 min. The resulting mixture was filtered, and the filtrate was concentrated in vacuo. The residue was purified by column chromatography (silica gel, 50−100% EtOAc/hexane) followed by preparative HPLC to give **3l** (12.5 mg, 0.0310 mmol, 24%) as a colorless oil. ^{1}H NMR (CDCl$_3$) δ 1.08−1.83 (5H, m), 2.43 (3H, s), 2.50−3.37 (5H, m), 4.25−4.45 (1H, m), 6.81−7.65 (9H, m), 8.23−8.61 (2H, m); MS (ESI) m/z: 405 (M + H)$^+$.

(4-Benzyl-4-hydroxypiperidin-1-yl)(5-methyl-2-(3-methylpyridin-4-yl)phenyl)methanone (3m). Compound **3m** (39.0 mg, 0.0970 mmol, 38%) was obtained as a colorless oil by a method similar to that described for **3k**. ^{1}H NMR (CDCl$_3$) δ 1.44 (2H, brs), 2.22 (4H, brs), 2.43 (4H, s), 2.52 (1H, brs), 2.69 (2H, s), 2.81−3.04 (1H, m), 3.16 (2H, brs), 4.31 (1H, d, J = 13.3 Hz), 6.99−7.39 (9H, m), 8.34−8.62 (2H, m); ^{13}C NMR (CDCl$_3$) δ 17.09, 21.15, 37.37, 42.84, 49.21, 69.14, 126.90, 128.44, 129.42, 129.50, 130.42, 135.72, 136.02, 138.62, 146.80, 147.09, 151.14, 168.79; MS (ESI) m/z: 401 (M + H)$^+$.

(4-Benzyl-4-hydroxypiperidin-1-yl)(3-methyl-2-(pyridin-4-yl)-phenyl)methanone (3n). A mixture of 2-bromo-3-methylbenzoic acid **4i** (300 mg, 1.40 mmol), DMT-MM (463 mg, 1.67 mmol), 4-benzylpiperidin-4-ol **9f** (267 mg, 1.40 mmol), N-methylmorpholine (0.767 mL, 6.98 mmol), and DMF (5.00 mL) was stirred at room temperature for 4 h. The mixture was quenched with water at room temperature and extracted with EtOAc. The organic layer was separated, washed with brine, dried over Na$_2$SO$_4$, and concentrated in vacuo. The resulting crude product, Pd(PPh$_3$)$_4$ (81.0 mg, 0.0700 mmol), sodium carbonate (297 mg, 2.80 mmol), pyridine-4-boronic acid **5a** (258 mg, 2.10 mmol), DME (5.00 mL), and water (1.00 mL) were heated at 140 °C under microwave irradiation for 1 h. The mixture was quenched with water at room temperature and extracted with EtOAc. The organic layer was separated, washed with brine, dried over Na$_2$SO$_4$, and concentrated in vacuo. The residue was purified by column chromatography (NH silica gel, 0−20% EtOAc/hexane) and by column chromatography (silica gel, 0−20% MeOH/hexane), followed by crystallization (EtOAc/hexane) to give **3n** (112 mg, 0.290 mmol, 20%) as a white solid. Mp 189 °C (EtOAc/hexane); ^{1}H NMR (CDCl$_3$) δ 0.64−1.52 (5H, m), 2.17 (3H, d, J = 15.9 Hz), 2.44−3.32 (5H, m), 4.25 (1H, d, J = 12.8 Hz), 7.01−7.58 (10H, m), 8.44−8.84 (2H, m); ^{13}C NMR (CDCl$_3$) δ 20.42, 20.60, 35.95, 36.41, 36.71, 37.07, 37.14, 42.84, 42.92, 49.13, 49.36, 68.99, 69.27, 123.73, 124.13, 124.38, 125.05, 126.91, 128.45, 128.56, 130.42, 130.92, 134.95, 135.31, 135.73, 135.95, 136.56, 136.77, 146.77, 149.55, 168.69; MS (ESI) m/z: 387 (M + H)$^+$.

(4-Benzyl-4-hydroxypiperidin-1-yl)(4-methyl-2-(pyridin-4-yl)-phenyl)methanone (3o). Compound **3o** (737 mg, 1.91 mmol, 82%) was obtained as a pink solid by a method similar to that described for **3n**. ^{1}H NMR (CDCl$_3$) δ 0.20−1.74 (6H, m), 2.43 (3H, s), 2.69 (2H, brs), 2.88−3.16 (2H, m), 4.43 (1H, brs), 6.92−7.60 (10H, m), 8.52−8.74 (2H, m); ^{13}C NMR (CDCl$_3$) δ 21.28, 35.80, 36.31, 36.88, 37.46, 42.53, 42.87, 49.08, 49.18, 68.88, 69.17, 123.24, 123.84, 126.86, 127.51, 127.75, 128.40, 129.56, 129.69, 129.79, 129.90, 130.39, 132.78, 133.08, 135.20, 135.65, 135.72, 135.88, 139.52, 139.62, 147.75, 149.81, 169.04; MS (ESI) m/z: 387 (M + H)$^+$.

(4-Benzyl-4-hydroxypiperidin-1-yl)(2-methyl-6-(pyridin-4-yl)-phenyl)methanone (3p). To a mixture of 2-bromo-6-methylbenzoic acid **4k** (300 mg, 1.40 mmol), DMF (10.8 μl, 0.14 mmol), and THF (5.00 mL) was added oxalyl chloride (0.134 mL, 1.53 mmol) at 0 °C. The mixture was stirred at 0 °C to room temperature for 4 h. The mixture was concentrated in vacuo, and the residue was dissolved in THF (2.00 mL). This solution was added to a mixture of 4-benzylpiperidin-4-ol **9f** (295 mg, 1.54 mmol), triethylamine (0.893

mL, 6.42 mmol), and THF (5.00 mL) at room temperature. The mixture was stirred at the same temperature overnight. The solvent was removed in vacuo, and the obtained compound was dissolved in a microwave vessel with DME (5.00 mL). To this mixture was added Pd(PPh$_3$)$_4$ (74.0 mg, 0.0600 mmol), sodium carbonate (271 mg, 2.56 mmol), pyridine-4-boronic acid **5a** (236 mg, 1.92 mmol), and water (1.00 mL) and the resulting mixture was heated at 140 °C under microwave irradiation for 1 h. The mixture was quenched with water at room temperature and extracted with EtOAc. The organic layer was separated, washed with brine, dried over Na$_2$SO$_4$, and concentrated in vacuo. The residue was purified by column chromatography (NH silica gel, 0−20% EtOAc/hexane) followed by column chromatography (silica gel, 0−20% MeOH/ EtOAc) to give **3p** (283 mg, 0.732 mmol, 57%) as a colorless oil. ^{1}H NMR (CDCl$_3$) δ 0.34−2.10 (5H, m), 2.19−2.81 (6H, m), 2.86−3.16 (2H, m), 4.36−4.53 (1H, m), 6.93−7.75 (10H, m), 8.49−8.77 (2H, m); ^{13}C NMR (CDCl$_3$) δ 19.27, 19.37, 35.87, 36.45, 36.47, 36.95, 37.03, 37.25, 42.20, 42.29, 49.08, 49.15, 68.92, 69.11, 123.46, 124.08, 126.62, 126.88, 126.91, 128.42, 128.88, 128.90, 130.35, 130.41, 130.80, 135.08, 135.34, 135.29, 135.70, 135.87, 147.96, 148.09, 149.60, 149.69, 168.01, 168.04; MS (ESI) m/z: 387 (M + H)$^+$.

(4-Benzyl-4-hydroxypiperidin-1-yl)(2-(pyridin-4-yl)phenyl)-methanone (3t). Compound **3t** (763 mg, 2.05 mmol, 82%) was obtained as a pink solid by a method similar to that described for **3n**. ^{1}H NMR (CDCl$_3$) δ 0.11−1.85 (5H, m), 2.25−3.31 (5H, m), 4.43 (1H, brs), 6.77−7.81 (11H, m), 8.40−8.84 (2H, m); ^{13}C NMR (CDCl$_3$) δ 35.80, 36.32, 36.86, 37.47, 42.50, 42.86, 49.08, 49.18, 68.87, 69.15, 123.25, 123.86, 126.89, 127.45, 127.72, 128.42, 128.99, 129.13, 129.25, 129.51, 129.57, 130.37, 135.22, 135.60, 135.70, 135.91, 147.58, 149.81, 149.87, 168.77; MS (ESI) m/z: 373 (M + H)$^+$.

(4-Benzyl-4-hydroxypiperidin-1-yl)(2,4′-bipyridin-3-yl)-methanone (3v). A mixture of **10h** (5.00 g, 15.1 mmol), pyridine-4-boronic acid **5a** (2.23 g, 18.1 mmol), sodium carbonate (4.81 g, 45.3 mmol), Pd(PPh$_3$)$_4$ (0.873 g, 0.76 mmol), DMF (50 mL), and water (10 mL) was heated at 100 °C under N$_2$ overnight. To the reaction mixture, brine was added and extracted with EtOAc. The organic layer was separated, washed with brine, dried over Na$_2$SO$_4$, and concentrated in vacuo. The residue was purified by column chromatography (NH silica gel, 50−100% EtOAc/hexane) to give **3v** (3.42 g, 9.16 mmol, 61%) as a white solid. Crystallization from EtOAc/hexane afforded compound **3v** as a white crystal. Mp 150 °C (EtOAc/hexane); ^{1}H NMR (CDCl$_3$) δ 0.07-1.67 (5H, m), 2.35−3.17 (5H, m), 4.41−4.60 (1H, m), 6.98−7.15 (2H, m), 7.22−7.32 (3H, m), 7.41 (1H, dd, J = 7.5, 5.0 Hz), 7.61 (1H, d, J = 4.2 Hz), 7.70−7.83 (2H, m), 8.60−8.82 (3H, m); ^{13}C NMR (CDCl$_3$) δ 35.6, 36.0, 36.2, 36.7, 37.6, 42.5, 43.0, 49.1, 49.2, 68.8, 69.0, 122.8, 123.5, 126.9, 128.4, 130.3, 131.5, 131.8, 135.4, 135.6, 136.0, 136.1, 146.3, 150.0, 150.3, 151.6, 152.2, 167.2, 167.4; MS (ESI) m/z: 374 (M + H)$^+$; Anal. Calcd for C$_{23}$H$_{23}$N$_3$O$_2$: C, 73.97; H, 6.21; N, 11.25. Found: C, 73.81; H, 6.27; N, 11.15.

2,4′-Bipyridin-3-yl(4-hydroxy-4-(pyridin-2-ylmethyl)piperidin-1-yl)methanone (3y). A solution of 2-chloronicotinic acid **4m** (150 mg, 0.950 mmol), HATU (434 mg, 1.14 mmol), triethylamine (0.663 mL, 4.76 mmol), and 4-(pyridin-2-ylmethyl)piperidin-4-ol dihydrochloride **9k** (201 mg, 1.05 mmol) in DMF (5.00 mL) was stirred at room temperature for 4 h. The mixture was quenched with water at room temperature and extracted with EtOAc. The organic layer was separated, washed with brine, dried over Na$_2$SO$_4$, and concentrated in vacuo. The resulting crude product (**10i**), Pd(PPh$_3$)$_4$ (54.9 mg, 0.0500 mmol), sodium carbonate (201 mg, 1.90 mmol), pyridine-4-boronic acid **5a** (128 mg, 1.05 mmol), DME (5.00 mL), and water (1.00 mL) were heated at 140 °C for 1 h under microwave irradiation. The mixture was quenched with water at room temperature and extracted with EtOAc. The organic layer was separated, washed with brine, dried over Na$_2$SO$_4$, and concentrated in vacuo. The residue was purified by column chromatography (NH silica gel, 50−80% EtOAc/ hexane) to give **3y** (116 mg, 0.310 mmol, 33%) as a colorless oil. ^{1}H NMR (CDCl$_3$) δ 0.84−1.58 (5H, m), 2.43−3.36 (5H, m), 4.49 (1H, d, J = 10.6 Hz), 7.00−7.10 (1H, m), 7.12−7.21 (1H, m), 7.35−7.47 (1H, m), 7.56−7.68 (2H, m), 7.77 (2H, d, J = 5.3 Hz), 8.42 (1H, d, J = 4.9 Hz), 8.66−8.80 (3H, m); MS (ESI) m/z: 375 (M + H)$^+$.

tert-Butyl 4-(2-bromo-5-methylbenzoyl)piperazine-1-carboxylate (11). A mixture of **24h** (500 mg, 2.33 mmol), DIPEA (0.609 mL, 3.49 mmol), HATU (1.06 g, 2.79 mmol), *tert*-butylpiperazine-1-carboxylate (520 mg, 2.79 mmol), and DMF (5.00 mL) was stirred at room temperature overnight. The reaction mixture was diluted with water and extracted with EtOAc. The extract was washed with water and brine, dried over MgSO$_4$, filtered, and concentrated in vacuo. The residue was purified by column chromatography (silica gel, 20−50% EtOAc/hexane) to give **11** (877 mg, 2.29 mmol, 98%) as a white solid. ^{1}H NMR (CDCl$_3$) δ 1.47 (9H, s), 2.32 (3H, s), 3.10−3.61 (6H, m), 3.65−3.90 (2H, m), 7.01−7.11 (2H, m), 7.39−7.50 (1H, m).

(5-Methyl-2-(pyridin-4-yl)phenyl)(piperazin-1-yl)methanone (12). A mixture of **11** (500 mg, 1.30 mmol), Pd(PPh$_3$)$_4$ (75.0 mg, 0.0700 mmol), sodium carbonate (277 mg, 2.61 mmol), pyridine-4-boronic acid **5a** (176 mg, 1.43 mmol), DME (10.0 mL), and water (2.00 mL) was heated at 150 °C for 1 h under microwave irradiation. The mixture was quenched with water at room temperature and extracted with EtOAc. The organic layer was separated, washed with brine, dried over MgSO$_4$, and concentrated in vacuo. The residue was purified by column chromatography (silica gel, 50−100% EtOAc/ hexane). A solution of this crude compound in EtOAc (5.00 mL) was added to 4 M HCl solution of EtOAc (5.00 mL, 20.0 mmol) at room temperature. The mixture was stirred at the same temperature overnight, and concentrated in vacuo. The residue was dissolved with water and washed with EtOAc. The aqueous layer was basified with 1 M NaOH, diluted with brine, and extracted with EtOAc−THF. The extract was washed with brine, dried over MgSO$_4$, filtered, and concentrated in vacuo to give **12** (283 mg, 1.01 mmol, 78%) as a colorless oil. ^{1}H NMR (CDCl$_3$) δ 1.43 (1H, s), 1.93 (1H, ddd, J = 11.5, 7.8, 3.0 Hz), 2.42 (3H, s), 2.44−2.60 (2H, m), 2.64−2.85 (2H, m), 2.89−3.03 (1H, m), 3.48−3.66 (2H, m), 7.24 (1H, d, J = 0.8 Hz), 7.30−7.34 (2H, m), 7.38−7.43 (2H, m), 8.57−8.68 (2H, m); MS (ESI) m/z: 282 (M + H)$^+$.

(4-Benzylpiperazin-1-yl)(5-methyl-2-(pyridin-4-yl)phenyl)-methanone (3b). To a mixture of **12** (50.0 mg, 0.180 mmol) and benzaldehyde (0.0220 mL, 0.210 mmol) in EtOAc (2.00 mL) was added NaBH(OAc)$_3$ (56.5 mg, 0.270 mmol) at room temperature. The mixture was stirred at the same temperature overnight. Then the mixture was quenched with water, diluted with 1 M NaOH, and extracted with EtOAc. The organic layer was separated, washed with brine, dried over MgSO$_4$, and concentrated in vacuo. The residue was purified by column chromatography (NH silica gel, 10−50% EtOAc/ hexane) to give **3b** (60.6 mg, 0.163 mmol, 92%) as a colorless oil. ^{1}H NMR (CDCl$_3$) δ 1.52 (1H, t, J = 7.6 Hz), 2.01−2.19 (2H, m), 2.31−2.45 (4H, m), 2.66−2.77 (1H, m), 2.94−3.05 (1H, m), 3.31 (2H, s), 3.47−3.71 (2H, m), 7.17−7.26 (5H, m), 7.27−7.32 (3H, m), 7.37−7.41 (2H, m), 8.59−8.66 (2H, m); MS (ESI) m/z: 372 (M + H)$^+$.

(4-Benzoylpiperazin-1-yl)(5-methyl-2-(pyridin-4-yl)phenyl)-methanone (3c). A mixture of **12** (50.0 mg, 0.180 mmol), benzoic acid (26.0 mg, 0.210 mmol), HATU (101 mg, 0.270 mmol), DIPEA (0.0930 mL, 0.530 mmol), and DMF (1.00 mL) was stirred at room temperature overnight. The reaction mixture was diluted with water and extracted with EtOAc. The extract was washed with brine, dried over MgSO$_4$, and concentrated in vacuo. The residue was purified by column chromatography (NH silica gel, 50−100% EtOAc/hexane) and crystallized from EtOAc−hexane to give **3c** (50.3 mg, 0.130 mmol, 73%) as a white solid. Mp 184 °C (EtOAc/hexane); ^{1}H NMR (CDCl$_3$) δ 2.43 (3H, s), 2.56−4.01 (8H, m), 7.22−7.45 (10H, m), 8.60−8.70 (2H, m); ^{13}C NMR (CDCl$_3$) δ 21.11, 41.59, 46.38, 123.34, 126.98, 128.37, 128.59, 129.06, 130.06, 130.85, 132.79, 134.57, 134.95, 139.74, 147.21, 150.13, 169.56, 170.35; MS (ESI) m/z: 386 (M + H)$^+$.

Protein Crystallization and Structure Analyses. Human CH24H (aa 28-494) with an N-terminal 6xHIS tag was cloned into pCWOri vector (Addgene). The above plasmid was co-transformed together with pGro7 (TaKaRa) into *E. coli* stain DH5α. To express the protein, the transformed cells were cultured in 2XYT media and induced at OD 0.8−1 with 1 mM IPTG, 0.5 mM 5-aminolevulinic

acid hydrochloride, and 0.02% arabinose, and then further cultured at 30 °C for 72 h. The cells were harvested and purified.[34] The final protein concentration for crystallization was 28 mg in the buffer containing 50 mM KPi 7.4, 500 mM NaCl, 0.5 mM EDTA, 2 mM DTT, and 10% glycerol. The CH24H co-crystal complex was prepared by addition of 2 mM compound and grown from a reservoir solution containing 0.4 M calcium chloride and 18% (w/v) PEG 3350 at 20 °C by the sitting-drop vapor diffusion method. Prior to data collection, crystals were immersed in the reservoir solution containing 25% ethylene glycol as a cryoprotectant and flash-frozen in liquid nitrogen. Diffraction data were collected from a single crystal using the CCD detector Quantum 315R (ADSC) at beamline 5.0.3 of the Advanced Light Source (Berkeley, CA) under a 100 K nitrogen cryostream. The data were reduced and scaled with the program HKL2000.[35] The structure was solved by the molecular replacement method with Molrep[36] of the CCP4 program suites[37] using the CH24H structure (PDB code 2Q9F) as a search model. The structure was refined through an iterative procedure utilizing REFMAC[38] followed by interactive model building using the program COOT.[39] The dictionary files for the ligands were prepared using AFITT (OpenEye Scientific Software). The final models were validated using MolProbity.[40] Crystallographic processing and refinement statistics are summarized in Supplementary Table 4. All graphical figures were generated using PyMOL (Schrödinger LLC, Cambridge, MA) and LIGPLOT.[41]

Measurement of CH24H Inhibitory Activity. CH24H enzyme was expressed by transducing full-length CH24H gene (NCBI Accession Num. BC022539) into FreeStyle 293-F cells (Invitrogen, Carlsbad, CA). A CH24H lysate product was prepared from supernatant isolated by centrifugation of the homogenate. Catalytic activity of CH24H enzyme was measured using TLC. To evaluate the inhibitory activity, 2 μL of serial diluted compounds were incubated with 3 μL of CH24H enzyme in assay buffer (50 mM Potassium phosphate buffer (pH 7.4) supplemented with 0.1% BSA and Complete EDTA-free (Roche, Switzerland)) for about 15 min at room temperature. The final concentration of DMSO in the assay was 0.2% when the compound was tested in duplicate in 384-well plates. The reaction was started with the addition of 5 μL of substrate [14C] Cholesterol (PerkinElmer, Foster City, CA, NEC018250UC) at a final concentration of 15 μM, which was dissolved in assay buffer containing 2 mM β-NADPH. After 5-h incubation at 37 °C, 35 μL of chloroform: methanol (1:2 v/v) was added to terminate the CH24H reaction. After mixing, 25 μL of distilled water containing 0.0024% Trypan blue was added to the mixture. Based on the Bligh and Dyer total lipid extraction method, 4.5 μL of the lower layer was spotted on the TLC plate. The TLC plates were developed using ethyl acetate:toluene (2:3 v/v) and visualized by FLA7000 (Fujifilm Corporation, Japan).

Measurement of CYP3A4 Inhibitory Activity. Incubation mixtures were prepared in a total volume of 40 μL with final component concentrations as follows: 50 mmol/L phosphate buffer (pH 7.4), NADPH-generating system (a mixture of MgCl$_2$, β-NADP$^+$, glucose-6-phosphate, and glucose-6-phosphate dehydrogenase), CYP3A4-expressing microsome (BD Biosciences), substrate (testosterone), and 10 μmol/L test compounds. The substrate and inhibitors were dissolved in methanol and dimethylsulfoxide, respectively, and added to the incubation mixture with the final solvent concentration of 0.5%. Incubations were conducted for 60 min and terminated by adding acetonitrile. After centrifugation, aliquots of the supernatants were subjected to measurement of the LC/MS/MS. All incubations were made in triplicate. The activity of CYP3A4 was determined by the peak of 6β-hydroxytestosterone. The activities of test samples were expressed as the percentage of activity remaining compared with a control sample containing no inhibitor.

Measurement of CYP Family Enzyme Inhibitory Activity. Incubation mixtures were prepared in a total volume of 100 μL with final component concentrations as follows: 50 mmol/L phosphate buffer (pH 7.4), NADPH-generating system (a mixture of MgCl$_2$, β-NADP$^+$, glucose-6-phosphate, and glucose-6-phosphate dehydrogenase), CYP-expressing microsomes (CYP1A2, CYP2C8, CYP2C9, CYP2C19, CYP2D6, or CYP3A4; BD Biosciences), substrates (phenacetin, amodiaquine, tolbutamide, (S)-mephenytoin, bufuralol, or testosterone), and 1–100 μmol/L test compounds. The substrates and inhibitors were dissolved in methanol and dimethylsulfoxide, respectively, and added to the incubation mixture with the final solvent concentration of 0.5%. Incubations were conducted at 37 °C for 10−20 min and terminated by adding acetonitrile. After centrifugation, aliquots of the supernatants were subjected to measurement of the LC/MS/MS. All incubations were made in duplicate. The activities of CYP1A2, CYP2C8, CYP2C9, CYP2C19, CYP2D6, and CYP3A4 were determined by the peak of acetaminophen, N-desethylamodiaquine, 1′-hydroxydiclofenac, 4′-hydoroxymephenytoin, 1′-hydroxybufuralol, and 6β-hydroxytestosterone, respectively. The activities of test samples were expressed as the percentage of activity remaining compared with a control sample containing no inhibitor.

In Vitro Steroidogenic Disruption Model in H295R Cells. The H295R human adrenocortical carcinoma cell line was obtained from American Type Culture Collection (ATCC, #CRL-2128). Cells were cultured in 75 mL flasks (Corning Costar, Cambridge, MA, 430641), with 30 mL of media at 37 °C with a 5% CO$_2$ atmosphere. Briefly, cells were grown in Dulbecco's modified Eagle's medium and Ham's F-12 Nutrient mixture (DMEM/F12) medium (COSMO-BIO, Tokyo, Japan, 16007100) supplemented with 2.5% Nu-serum (BD Falcon, Franklin, Lakes, NJ, 355100), 1% ITS-plus (BD Falcon, 354352), 100 units/mL penicillin, and 100 μg/mL streptomycin (Gibco, Grand Island, New York, 15140-122). The H295R steroid hormones synthesis assay was performed as follows: The cells were grown in 24-well plates (Corning Costar, 3526) with 5×10^4 cells in 0.5 mL of medium for each well, and were incubated three overnights. After incubation, the medium was changed with 0.5 mL of culture medium containing 20 μM forskolin. After two additional overnight incubations, cells were washed with 500 μL of DMEM/F12 medium supplemented with 1% ITS-plus twice. And then, the cells were treated with 500 μL of DMEM/F12 medium supplemented with 1% ITS-plus 20 μM forskolin and varying concentrations of the compounds. After overnight incubation, the supernatant of the culture media was collected and stored at −30 °C. Commercially available enzyme immunoassay (EIA) kits were used with steroid hormones, such as cortisol, testosterone, aldosterone, and corticosterone (Cayman, San Diego, CA, 500360, 582701, 10004377, and 500655, respectively), according to the manufacturer's instructions. The procedure followed the basic principle of EIA, in which there is competition between an acetylcholinesterase-linked hormone (tracer) and a nonradioactive hormone for a fixed number of antibody binding sites. Amounts of hormones in the above reserved cell culture media were quantitatively measured in the use of a calibration curve. Percentage inhibition was calculated from amounts of hormones using the following formula: % inhibition = $(A − X) \times 100/(A)$

A: 20 μM forskolin, X: 20 μM forskolin plus test inhibitor. IC$_{50}$ values were calculated with XLfit software (IDBS, Emeryville, CA) using a four-parameter logistic curve. Data are provided as the average and standard error of mean (SEM) performed in triplicate.

In Vitro Metabolic Clearance in Human Hepatic Microsomes. Human liver microsomes were purchased from Sekisui XenoTech, LLC. (Kansas City, KS). The microsomes (0.2 mg protein/mL) and the compound (1 μM) were mixed in phosphate buffer (pH 7.4). The reactions were initiated by adding an NADPH-generating system (a mixture of MgCl$_2$, glucose-6-phosphate, β-NADP$^+$, and glucose-6-phosphate dehydrogenase) to the mixtures before incubation. Incubations were conducted at 37 °C for 15 and 30 min and terminated by adding acetonitrile. The zero-time incubations, which served as the controls, were terminated by adding acetonitrile before adding each compound. After the samples were mixed and centrifuged, the compound concentrations in the supernatant fractions were measured by LC/MS/MS.

Ethics Statement. The care and use of the animals and the experimental protocols used in this research were approved by the Experimental Animal Care and Use Committee of Takeda Pharmaceutical Company Limited.

In Vivo PK/PD Study of Compound 3v in Mice. Female C57BL/6N mice (7- to 8-week-old) (3 mice/group) were used. Compound **3v** was suspended in a 0.5% aqueous methylcellulose [133-14255 WAKO] solution (10 mL/kg). The solution was forcibly administered orally at 1, 3, and 10 mg/kg. At 0.5 and 1, 2, 4, 8, and 24 h for 1 and 3 mg/kg, and at 0.25, 0.5, 1, 2, 4, 8, and 24 h for 10 mg/kg after administration, the animals were sacrificed and the brain samples were collected. The brain was homogenized with about 4-fold amount of saline. The concentrations of **3v** in the brain were measured with LC-MS/MS, and the brain 24HC was measured with HPLC described below.

Measurement of Plasma and Brain Concentrations of Compound 3v in Mice. The aliquots of the brain homogenate were mixed with acetonitrile containing internal standard. The mixtures were centrifuged. The supernatants were diluted with solvents for LC-MS/MS (mobile phase A: 10 mM ammonium formate/formic acid (100/0.2, v/v), mobile phase B: acetonitrile/formic acid (100/0.2, v/v)). The diluted solutions were injected into LC-MS/MS (API5000, AB Sciex, CA) equipped with Shimadzu Shim-pack XR-ODS (2.2 μm, 2.0 × 30 mm, Shimadzu Corporation, Japan) at 50 °C. Compound **3v** was detected using a multiple reaction monitoring mode using the transition: m/z 374.20 → 183.10. Analyst software TM (version 1.4.2) was used for data acquisition and processing.

Measurement of 24HC in the Mouse Brain. 24HC in the brain homogenate was extracted with an acetonitrile solution (98% acetonitrile, 1.98% methanol, 0.02% formic acid), and quantified by HPLC (UPLC, Waters corporation, MA) that was equipped with Acquity UPLC HSS C_{18} SB (1.8 μm, 2.1 × 100 mm) maintained at 40 °C. The average value of 24HC amount was calculated and the results are shown in relative values with the control group as 100%. UV detection was performed at 201 nm.

■ ASSOCIATED CONTENT

ⓢ Supporting Information

The Supporting Information is available free of charge at https://pubs.acs.org/doi/10.1021/acs.jmedchem.1c00864.

> X-ray data collection and refinement statistics for the crystal structures of CH24H in complex with compounds **1b**, **3f**, and **3v**; brain concentration of compound **3v** after oral administration in C57BL/6N mice (8 weeks) and the effect on 24HC reduction; chromatograms for purification and analysis of **3a–z**; and ^{1}H and ^{13}C NMR charts for **3v** (PDF)
>
> Molecular formula strings (CSV)

Accession Codes

The coordinates of the crystal structures of CH24H in complex with compounds **1b** (7LS4), **3f** (7LS3), and **3v** (7LRL) have been deposited in the Protein Data Bank. The authors will release the atomic coordinates and experimental data upon article publication.

■ AUTHOR INFORMATION

Corresponding Author

Tatsuki Koike – *Research, Takeda Pharmaceutical Company Ltd., Fujisawa, Kanagawa 251-8555, Japan;* ⓞ orcid.org/0000-0002-3264-1406; Phone: +81-466-32-1132; Email: tatsuki.koike@takeda.com

Authors

Masato Yoshikawa – *Research, Takeda Pharmaceutical Company Ltd., Fujisawa, Kanagawa 251-8555, Japan;* ⓞ orcid.org/0000-0002-7175-1173

Haruhi Kamisaki Ando – *Research, Takeda Pharmaceutical Company Ltd., Fujisawa, Kanagawa 251-8555, Japan*

William Farnaby – *Research, Takeda Pharmaceutical Company Ltd., Fujisawa, Kanagawa 251-8555, Japan*

Toshiya Nishi – *Research, Takeda Pharmaceutical Company Ltd., Fujisawa, Kanagawa 251-8555, Japan*

Etsurou Watanabe – *Research, Takeda Pharmaceutical Company Ltd., Fujisawa, Kanagawa 251-8555, Japan*

Jason Yano – *Takeda California Inc., San Diego, California 92121, United States*

Maki Miyamoto – *Research, Takeda Pharmaceutical Company Ltd., Fujisawa, Kanagawa 251-8555, Japan*

Shigeru Kondo – *Research, Takeda Pharmaceutical Company Ltd., Fujisawa, Kanagawa 251-8555, Japan*

Tsuyoshi Ishii – *Research, Takeda Pharmaceutical Company Ltd., Fujisawa, Kanagawa 251-8555, Japan*

Takanobu Kuroita – *Research, Takeda Pharmaceutical Company Ltd., Fujisawa, Kanagawa 251-8555, Japan*

Complete contact information is available at:
https://pubs.acs.org/10.1021/acs.jmedchem.1c00864

Author Contributions

The manuscript was written through contributions of all authors. All authors have given approval to the final version of the manuscript.

Notes

The authors declare the following competing financial interest(s): This study was funded by Takeda Pharmaceutical Company Limited (TAKEDA). T.K., M.Y., H.K.A, W.F., T.N., E.W., J.Y., M.M., S.K., T.I. and T.K. are current and former employees of TAKEDA. No other potential conflicts of interest relevant to this article exists.

■ ACKNOWLEDGMENTS

■ ABBREVIATIONS

AD, Alzheimer's disease; BBB, blood–brain barrier; CNS, central nervous system; CSF, cerebrospinal fluid; DDI, drug–drug interaction; HBA, hydrogen-bonding acceptor; HBD, hydrogen-bonding donor; 24HC, 24S-hydroxycholesterol; ^{1}H NMR, proton nuclear magnetic resonance; HTS, high-throughput screening; SAR, structure–activity relationship; SBDD, structure-based drug design; TLC, thin-layer chromatography

■ REFERENCES

(1) Russell, D. W.; Halford, R. W.; Ramirez, D. M.; Shah, R.; Kotti, T. Cholesterol 24-hydroxylase: An enzyme of cholesterol turnover in the brain. *Annu. Rev. Biochem.* **2009**, *78*, 1017−1040.

(2) Kölsch, H.; Lütjohann, D.; Ludwig, M.; Schulte, A.; Ptok, U.; Jessen, F.; von Bergmann, K.; Rao, M. L.; Maier, W.; Heun, R. Polymorphism in the cholesterol 24S-hydroxylase gene is associated with Alzheimer's disease. *Mol. Psychiatry* **2002**, *7*, 899−902.

(3) Li, L.; Yin, Z.; Liu, J.; Li, G.; Wang, Y.; Yan, J.; Zhou, H. CYP46A1 T/C polymorphism associated with the APOEepsilon4 allele increases the risk of Alzheimer's disease. *J. Neurol.* **2013**, *260*, 1701−1708.

(4) Schönknecht, P.; Lütjohann, D.; Pantel, J.; Bardenheuer, H.; Hartmann, T.; von Bergmann, K.; Beyreuther, K.; Schröder, J. 24S-hydroxycholesterol is increased in patients with Alzheimer's disease compared to healthy controls. *Neurosci. Lett.* **2002**, *324*, 83−85.

(5) Papassotiropoulos, A.; Lutjohanm, D.; Bagli, M.; Locatelli, S.; Jessen, F.; Buschfort, R.; Ptok, U.; Bjorkhem, I.; Bergmann von, K.; Heun, R. 24S-hydroxycholesterol in cerebrospinal fluid is elevated in early stages of dementia. *J. Psychiatr. Res.* **2002**, *36*, 27−32.

(6) Leoni, V.; Shafaati, M.; Salomon, A.; Kivipelto, M.; Björkhem, I.; Wahlund, L. O. Are the CSF levels of 24S-hydroxycholesterol a sensitive biomarker for mild cognitive impairment? *Neurosci. Lett.* **2006**, *397*, 83−87.

(7) Tian, G.; Kong, Q.; Lai, L.; Ray-Chaudhury, A.; Lin, C.-L. G. Increased expression of cholesterol 24S-hydroxylase results in disruption of glial glutamate transporter EAAT2 association with lipid rafts: a potential role in Alzheimer's disease. *J. Neurochem.* **2010**, *113*, 978−989.

(8) Nishi, T.; Kondo, S.; Miyamoto, M.; Watanabe, S.; Hasegawa, S.; Kondo, S.; Yano, J.; Watanabe, E.; Ishi, T.; Yoshikawa, M.; Ando, H. K.; Farnaby, W.; Fujimoto, S.; Sunahara, E.; Ohori, M.; During, M. J.; Kuroita, T.; Koike, T. Soticlestat, a novel cholesterol 24-hydroxylase inhibitor shows a therapeutic potential for neural hyperexcitation in mice. *Sci. Rep.* **2020**, *10*, No. 17081.

(9) Lehmann, J. M.; Kliewer, S. A.; Moore, L. B.; Smith-Oliver, T. A.; Oliver, B. B.; Su, J. L.; Sundseth, S. S.; Winegar, D. A.; Blanchard, D. E.; Spencer, T. A.; Willson, T. M. Activation of the nuclear receptor LXR by oxysterols defines a new hormone response pathway. *J. Biol. Chem.* **1997**, *272*, 3137−3140.

(10) Umetani, M.; Domoto, H.; Gormley, A. K.; Yuhanna, I. S.; Cummins, C. L.; Javitt, N. B.; Korach, K. S.; Shaul, P. W.; Mangelsdorf, D. J. 27-Hydroxycholesterol is an endogenous SERM that inhibits the cardiovascular effects of estrogen. *Nat. Med.* **2007**, *13*, 1185−1192.

(11) Wang, Y.; Kumar, N.; Crumbley, C.; Griffin, P. R.; Burris, T. P. A second class of nuclear receptors for oxysterols: Regulation of RORalpha and RORgamma activity by 24S-hydroxycholesterol (cerebrosterol). *Biochim. Biophys. Acta, Mol. Cell Biol. Lipids* **2010**, *1801*, 917−923.

(12) Paul, S. M.; Doherty, J. J.; Robichaud, A. J.; Belfort, G. M.; Chow, B. Y.; Hammond, R. S.; Crawford, D. C.; Linsenbardt, A. J.; Shu, H. J.; Izumi, Y.; Mennerick, S. J.; Zorumski, C. F. The major brain cholesterol metabolite 24(S)-hydroxycholesterol is a potent allosteric modulator of N-methyl-D-aspartate receptors. *J. Neurosci.* **2013**, *33*, 17290−300.

(13) Björkhem, I.; Lövgren-Sandblom, A.; Leoni, V.; Meaney, S.; Brodin, L.; Salveson, L.; Winge, K.; Pålhagen, S.; Svenningsson, P. Oxysterols and Parkinson's disease: evidence that levels of 24S-hydroxycholesterol in cerebrospinal fluid correlates with the duration of the disease. *Neurosci. Lett.* **2013**, *555*, 102−105.

(14) Boussicault, L.; Alves, S.; Lamazière, A.; Planques, A.; Heck, N.; Moumné, L.; Despres, G.; Bolte, S.; Hu, A.; Pagès, C.; Galvan, L.; Piguet, F.; Aubourg, P.; Cartier, N.; Caboche, J.; Betuing, S. CYP46A1, the rate-limiting enzyme for cholesterol degradation, is neuroprotective in Huntington's disease. *Brain* **2016**, *139*, 953−970.

(15) Djelti, F.; Braudeau, J.; Hudry, E.; Dhenain, M.; Varin, J.; Bièche, I.; Marquer, C.; Chali, F.; Ayciriex, S.; Auzeil, N.; Alves, S.; Langui, D.; Potier, M. C.; Laprevote, O.; Vidaud, M.; Duyckaerts, C.;

Miles, R.; Aubourg, P.; Cartier, N. CYP46A1 inhibition, brain cholesterol accumulation and neurodegeneration pave the way for Alzheimer's disease. *Brain* **2015**, *138*, 2383−2398.

(16) Hudry, E.; Van Dam, D.; Kulik, W.; De Deyn, P. P.; Stet, F. S.; Ahouansou, O.; Benraiss, A.; Delacourte, A.; Bougnères, P.; Aubourg, P.; Cartier, N. Adeno-associated virus gene therapy with cholesterol 24-hydroxylase reduces the amyloid pathology before or after the onset of amyloid plaques in mouse models of Alzheimer's disease. *Mol. Ther.* **2010**, *18*, 44−53.

(17) Mast, N.; Saadane, A.; Valencia-Olvera, A.; Constans, J.; Maxfield, E.; Arakawa, H.; Li, Y.; Landreth, G.; Pikuleva, I. A. Cholesterol-metabolizing enzyme cytochrome P450 46A1 as a pharmacologic target for Alzheimer's disease. *Neuropharmacology* **2017**, *123*, 465−476.

(18) Mast, N.; Verwilst, P.; Wilkey, C. J.; Guengerich, F. P.; Pikuleva, I. A. In Vitro Activation of Cytochrome P450 46A1 (CYP46A1) by Efavirenz-Related Compounds. *J. Med. Chem.* **2020**, *63*, 6477−6488.

(19) Petrov, A. M.; Lam, M.; Mast, N.; Moon, J.; Li, Y.; Maxfield, E.; Pikuleva, I. A. CYP46A1 Activation by Efavirenz Leads to Behavioral Improvement without Significant Changes in Amyloid Plaque Load in the Brain of 5XFAD Mice. *Neurotherapeutics* **2019**, *16*, 710−724.

(20) Bialer, M.; Johannessen, S. I.; Koepp, M. J.; Levy, R. H.; Perucca, E.; Tomson, T.; White, H. S. Progress report on new antiepileptic drugs: A summary of the Fourteenth Eilat Conference on New Antiepileptic Drugs and Devices (EILAT XIV). I. Drugs in preclinical and early clinical development. *Epilepsia* **2018**, *59*, 1811−1841.

(21) Strzelczyk, A.; Schubert-Bast, S. Therapeutic advances in Dravet syndrome: a targeted literature review. *Expert Rev. Neurother.* **2020**, *20*, 1065−1079.

(22) Halford, J. J.; Sperling, M. R.; Arkilo, D.; Asgharnejad, M.; Zinger, C.; Xu, R.; During, M.; French, J. A. A phase 1b/2a study of soticlestat as adjunctive therapy in participants with developmental and/or epileptic encephalopathies. *Epilepsy Res.* **2021**, *174*, No. 106646.

(23) Guengerich, F. P. Human Cytochrome P450 Enzymes. In *Cytochrome P450: Structure, Mechanism, and Biochemistry*, 3rd ed.; Ortiz de Montellano, P. R., Ed.; Kluwer Academic: New York, 2005; pp 377−530.

(24) Mast, N.; White, M. A.; Bjorkhem, I.; Jhonson, E. F.; Stout, C. D.; Pikuleva, I. A. Crystal structures of substrate-bound and substrate-free cytochrome P450 46A1, the principal cholesterol hydroxylase in the brain. *Proc. Natl. Acad. Sci. USA* **2008**, *105*, 9546−9551.

(25) Mast, N.; Charvet, C.; Pikuleva, I. A.; Stout, C. D. Structural basis of drug binding to CYP46A1, an enzyme that controls cholesterol turnover in the brain. *J. Biol. Chem.* **2010**, *285*, 31783−31795.

(26) Mast, N.; Linger, M.; Clark, M.; Wiseman, J.; Stout, C. D.; Pikuleva, I. A. *In silico* and intuitive predictions of CYP46A1 inhibition by marketed drugs with subsequent enzyme crystallization in complex with fluvoxamine. *Mol. Pharmacol.* **2012**, *82*, 824−834.

(27) Shafaati, M.; Mast, N.; Beck, O.; Nayef, R.; Heo, G. Y.; Björkhem-Bergman, L.; Lütjohann, D.; Björkhem, I.; Pikuleva, I. A. The antifungal drug voriconazole is an efficient inhibitor of brain cholesterol 24S-hydroxylase in vitro and in vivo. *J. Lipid Res.* **2010**, *51*, 318−323.

(28) Mast, N.; Zheng, W.; Stout, C. D.; Pikuleva, I. A. Antifungal Azoles: Structural Insights into Undesired Tight Binding to Cholesterol-Metabolizing CYP46A1. *Mol. Pharmacol.* **2013**, *84*, 86−94.

(29) Mast, N.; Zheng, W.; Stout, C. D.; Pikuleva, I. A. Binding of a cyano- and fluoro-containing drug bicalutamide to cytochrome P450 46A1: unusual features and spectral response. *J. Biol. Chem.* **2013**, *288*, 4613−4624.

(30) Leclerc, J. P.; Fagnou, K. Palladium-Catalyzed Cross-Coupling Reactions of Diazine *N*-Oxides with Aryl Chlorides, Bromides, and Iodides. *Angew. Chem., Int. Ed.* **2006**, *45*, 7781−7786.

(31) Leo, A.; Weininger, D. Clogp Reference Manual, Daylight, version 4.9. http://www.daylight.com/dayhtml/doc/clogp/.

(32) Nielsen, F. K.; Hansen, C. H.; Fey, J. A.; Hansen, M.; Jacobsen, N. W.; Halling-Sorensen, B.; Bjorklund, E.; Styrishave, B. H295R cells as a model for steroidogenic disruption: a broader perspective using simultaneous chemical analysis of 7 key steroid hormones. *Toxicol. In Vitro* **2012**, *26*, 343−350.

(33) Oskarsson, A.; Ullerås, E.; Plant, K. E.; Hinson, J. P.; Goldfarb, P. S. Steroidogenic gene expression in H295R cells and the human adrenal gland: adrenotoxic effects of lindane in vitro. *J. Appl. Toxicol.* **2006**, *26*, 484−492.

(34) White, M. A.; Mast, N.; Bjorkhem, I.; Johnson, E. F.; Stout, C. D.; Pikuleva, I. A. Use of complementary cation and anion heavy-atom salt derivatives to solve the structure of cytochrome P450 46A1. *Acta Crystallogr., Sect. D: Biol. Crystallogr.* **2008**, *64*, 487−495.

(35) Otwinowski, Z.; Minor, W. [20] Processing of X-ray diffraction data collected in oscillation mode. *Methods Enzymol.* **1997**, *276*, 307−326.

(36) Vagin, A.; Teplyakov, A. MOLREP: an Automated Program for Molecular Replacement. *J. Appl. Crystallogr.* **1997**, *30*, 1022−1025.

(37) Project CC Collaborative Computational Project, N The CCP4 suite: programs for protein crystallography *Acta Crystallogr., Sect. D: Biol. Crystallogr.* 1994, *50*, 760 763 DOI: 10.1107/S0907444994003112.

(38) Murshudov, G. N.; Skubák, P.; Lebedev, A. A.; Pannu, N. S.; Steiner, R. A.; Nicholls, R. A.; Winn, M. D.; Long, F.; Vagin, A. A. REFMAC5 for the refinement of macromolecular crystal structures. *Acta Crystallogr., Sect. D: Biol. Crystallogr.* **2011**, *67*, 355−367.

(39) Emsley, P.; Lohkamp, B.; Scott, W. G.; Cowtan, K. Features and development of Coot. *Acta Crystallogr., Sect. D: Biol. Crystallogr.* **2010**, *66*, 486−501.

(40) Chen, V. B.; Arendall, W. B., 3rd; Headd, J. J.; Keedy, D. A.; Immormino, R. M.; Kapral, G. J.; Murray, L. W.; Richardson, J. S.; Richardson, D. C. MolProbity: all-atom structure validation for macromolecular crystallography. *Acta Crystallogr., Sect. D: Biol. Crystallogr.* **2010**, *66*, 12−21.

(41) Wallace, A. C.; Laskowski, R. A.; Thornton, J. M. LIGPLOT: a program to generate schematic diagrams of protein-ligand interactions. *Protein Eng., Des. Sel.* **1995**, *8*, 127−134.

■ NOTE ADDED AFTER ASAP PUBLICATION

This article published August 13, 2021 with an incorrect Figure 5 file. The correct figure published August 16, 2021.